

1 **Global Sensitivity Analysis for Multiple Interpretive Models with Uncertain Parameters**

2

3 A. Dell'Oca, M. Riva, A. Guadagnini

4

5 Dipartimento di Ingegneria Civile e Ambientale (DICA), Politecnico di Milano, Piazza L. Da Vinci,

6 32, 20133 Milano, Italy

7

8

9

## Abstract

10 We propose a set of new indices to assist global sensitivity analysis (GSA) in the presence of data  
11 allowing for interpretations based on a collection of diverse models whose parameters could be  
12 affected by uncertainty. Our GSA metrics enable us to assess the sensitivity of various features (as  
13 rendered through statistical moments) of the probability density function of a quantity of interest  
14 with respect to imperfect knowledge of (i) the interpretive model employed to characterize the  
15 system behavior and (ii) the ensuing model parameters. We exemplify our methodology for the case  
16 of heavy metal sorption onto soil, for which we consider three broadly used (equilibrium isotherm)  
17 models. Our analyses consider (a) an unconstrained case, i.e., when no data are available to  
18 constrain parameter uncertainty and to evaluate the (relative) plausibility of each considered model,  
19 and (b) a constrained case, i.e., when the analysis is constrained against experimental observations.  
20 Our moment-based indices are structured according to two key components: (a) a model-choice  
21 contribution, associated with the possibility of analyzing the system of interest by taking advantage  
22 of multiple model conceptualizations (or mathematical renderings); and (b) a parameter-choice  
23 contribution, related to the uncertainty in the parameters of a selected model. Our results indicate  
24 that a given parameter can be associated with diverse degrees of importance, depending on the  
25 considered statistical moment of the target model output. The influence on the latter of parameter  
26 and model uncertainty evolves as a function of the available level of information about the modeled  
27 system behavior.

28

29

30

## Plain Language Summary

31 The quality and amount of data available in many practical situations justify the interpretation of the  
32 system under investigation through a collection of alternative interpretative models. This is  
33 reflected by the observation that there is uncertainty about model structure/format. The situation is  
34 exacerbated by the observation that parameters associated with each model could also be affected  
35 by uncertainty. In this context, quantification of the influence of these multiple sources of  
36 uncertainties on environmental quantities of interest is key to increase our understanding and  
37 confidence on model(s) functioning and guide further actions (including, e.g., model calibration or  
38 collection of new data). We propose an original Global Sensitivity Analysis (GSA) approach that  
39 enables us to quantify the sensitivity of a target quantity with respect to each of the parameters  
40 stemming from situations where multiple interpretative models have been formulated. The proposed  
41 GSA allows (i) investigating the sensitivity of model outputs through diverse aspects of uncertainty  
42 (i.e., focusing on various statistical moments of the probability density function of the target output)  
43 as well as (ii) discriminating between contributions to sensitivity due to our lack of knowledge in  
44 (a) model format and (b) parameter values.

45

46

## Highlights

- 47 • A novel Global Sensitivity Analysis in case of multiple alternative interpretive models is  
48 proposed.
- 49 • The approach allows discriminating between contributions to sensitivity due to our lack of  
50 knowledge in (a) model format and (b) parameter values.
- 51 • We analyze the evolution of the proposed sensitivity metrics as observations about the system  
52 under investigation become available.

## 1. Introduction

Sensitivity analysis is key to assist understanding (and eventually improvement) of models aiming at rendering the dynamics of environmental/hydrological systems. Challenges associated with a sensitivity analysis are exacerbated by the increasing complexity of conceptual models, in terms of model formulation and associated parametrization, which is in turn sustained by our increased knowledge of environmental dynamics and by the exponentially increasing computational power available for numerical model simulations (e.g., Paniconi and Putti, 2015; Förster et al., 2014; Herman et al., 2013; Wagener and Montanari, 2011; Koutsoyiannis, 2010). Sensitivity analysis techniques can be classified according to two categories, i.e., local and global methods (e.g., Gupta and Razavi, 2018; Pianosi et al. 2016; Borgonovo and Plischke, 2016; Razavi and Gupta, 2016a,b). According to the former approach, sensitivity (typically resting on the derivative concept) is evaluated in the neighborhood of a given combination of parameters of a model. Global sensitivity analysis (GSA) approaches rest on the evaluation of sensitivity (usually quantified through metrics entailing the variability of the model response) across the entire support within which model system parameters vary. As such, the typically encountered uncertainty about parameters driving the behavior of environmental/hydrological systems can be readily accommodated in this context (Saltelli et al., 2008). Our study is set within a GSA framework.

In this broad framework, it is important to note that the formal definition of a sensitivity metric must be linked to the nature of the question(s) the GSA is intended to address. Understanding of the way uncertainty associated with model parameters affects uncertainty of given modeling goals / results can be useful to address various research questions, such as: Which are the most important model parameters with respect to given model output(s) / response(s)? (e.g., Hill et al., 2016; Ruano et al., 2012; Wagner et al., 2009; Pappenberger et al., 2008; Gupta et al., 2008; Muleta and Nicklow, 2005); What are the relationships between key features of model output(s) uncertainty and model parameter(s)? (e.g., Pianosi and Wagner, 2015; Borgonovo, 2007; Liu et al., 2006); Could we set some parameter(s) (which are deemed as uninfluential) at prescribed value(s) without significantly affecting model results? (e.g., Chu et al., 2015; Punzo et al., 2015; Nossent et al., 2011; van Griensven et al., 2006; Degenring et al., 2004); At which space/time locations can one expect the highest sensitivity of model output(s) to model parameters and which parameter(s) data could be most beneficial for model calibration? (e.g., Hölder et al., 2018; Wang et al., 2018; Younes et al., 2016; Ciriello et al., 2015; Fajraoui et al., 2011; Yue et al., 2008).

Dell’Oca et al. (2017) focus on these research questions by proposing a moment-based GSA approach enabling quantification of the influence of uncertain model parameters on the (statistical) moments of a target model output. In this sense, these authors (*i*) define sensitivity in terms of the (average) variation of main statistical moments of the probability density function (*pdf*) of an output due to model parameter uncertainty and (*ii*) propose summary sensitivity indices (termed *AMA* indices after the Authors’ initials) to quantify the concept. Here, we extend the *AMA* indices to embed the effect of uncertainties both in the system model conceptualization and in the model(s) parameters. Our study rests on the observation that physical processes and natural systems within which they take place are complex, making state variables amenable to a multiplicity of interpretations and (conceptual/mathematical) descriptions, including system parameterizations. As such, predictions and uncertainty analyses based on a unique model can yield statistical bias and underestimation of uncertainty, thus justifying the assessment of multiple (competing) model system conceptualizations (e.g., Clark et al., 2008; Wholing and Vrugt, 2008; Ye et al., 2008a; Beven 2006; Poeter and Anderson, 2005; Bredehoeft, 2005; Burnham and Anderson, 2002). When a collection of alternative models is available, one can then use various criteria to (*a*) rank such models and/or (*b*) weigh model-based predictions (e.g., Höge et al., 2019; Neuman, 2012; Ye et al., 2008b, 2004; Neuman et al., 2003; Kass and Raftery, 1995). When prior information is unavailable, one can assign equal prior probability (or a priori model weight) to each model. Otherwise, a posterior model probability (or a posterior model weight) can be linked to each model when observations on the state variables of interest are made available (e.g., Rodríguez-Escales et al.,

104 2018; Höge et al., 2018; Liu et al., 2016; Knuth et al., 2015; Schöniger et al., 2014; Ye et al.,  
105 2008b).

106 In this context, the study of Dai and Ye (2015) highlights the importance of extending the  
107 classical variance-based GSA approach to include the possibility that a collection of models can be  
108 employed to assess a quantity of interest. In this multi-model framework, these authors introduce a  
109 definition of sensitivity that combines the model-averaging approach with the variance-based  
110 methodology to quantify an averaged (across the set of models) contribution of a parameter  
111 (including its interaction with other parameters) to a model-averaged variance of the output of  
112 interest. Dai et al. (2017) focus on the quantification (through a variance-based method) of the  
113 sensitivity of model prediction(s) to the uncertainty in the conceptualization of diverse model  
114 system processes, a setting corresponding to a lack of knowledge about the conceptualization of  
115 differing processes (and eventually their controlling parameters) contributing to a model structure.  
116 The GSA approach presented by Dai and Ye (2015) and Dai et al. (2017) is based on the rationale  
117 that the definition of sensitivity is that of uncertainty (as rendered through the variance)  
118 apportioning, i.e., the highest sensitivity is attributed to the factor providing the highest contribution  
119 to the uncertainty of the output of interest.

120 A key element distinguishing our study from those of Dai and Ye (2015) and Dai et al. (2017)  
121 is the definition of the metric employed to quantify sensitivity. Here, we identify sensitivity with the  
122 (average) variation of a set of statistical moments of the *pdf* of a desired output (thus considering  
123 various features of the uncertainty on the output) due to the uncertainty on (a) the conceptualization  
124 of the system functioning (as rendered through various alternative model formulations) and (b)  
125 model parameters. In this sense, our definition of sensitivity is more relevant for factor fixing  
126 aspects (i.e., with reference to questions of the kind “How does a parameter affect a given statistical  
127 moment of the output *pdf*?” and/or “Is it possible to fix its value arbitrarily?”), rather than for the  
128 uncertainty apportioning aspect. A comparison between the metrics at heart of our GSA approach  
129 and those proposed by Dai and Ye (2015) and Dai et al. (2017) is provided in Appendix B-C.

130 Following the idea of uncertainty apportioning, Baroni and Tarantola (2014) present a  
131 probabilistic framework for uncertainty and global sensitivity analysis focusing on hydrological  
132 studies. These authors distinguish five sources of uncertainty, respectively corresponding to model  
133 input (e.g., weather data), time-varying model parameters (e.g., crop height), scalar model  
134 parameters (e.g., soil hydraulic properties), available observations (e.g., soil moisture), and model  
135 structure. With reference to the latter, these authors identify model structure uncertainty with the  
136 use of diverse levels of (space-time) refinement and descriptive detail of an otherwise  
137 deterministically given mathematical model, i.e., they do not analyze the impact of considering a set  
138 of alternative conceptual/mathematical formulations to render the investigated system. A GSA is  
139 then performed upon relying on the Sobol indices. In a similar fashion, Schoups and Hopmans  
140 (2006) present a sensitivity analysis methodology aimed at assessing the relative importance of  
141 three common sources of uncertainty, i.e., parameters, observation error and the model structure,  
142 here encompassing both the level of model refinement/details and the format of the  
143 conceptual/mathematical formulation), and measurements error, by focusing on the fractional  
144 contribution of each of these sources to the total predictive error between observations and  
145 corresponding model outputs. As mentioned above, our multi-model GSA is guided by a diverse  
146 rationale.

147 We exemplify our approach by targeting a geochemical phenomenon associated with the  
148 process of sorption of single metal onto a soil and considering three differing models that are  
149 typically used in the literature, each associated with uncertain parameters. We structure our analyses  
150 across two stages. We start in the absence of data/observations on the target model output against  
151 which one would perform model calibration (i.e., an equal prior probability is assigned to each  
152 candidate model and uncertainty of each model parameters is rendered through uniform *pdfs*  
153 characterized by the same coefficient of variation). In this case, the purpose of a GSA is that of (i)  
154 improving our understanding of the model functioning, in terms of the relevance of each model

155 parameter on the considered model output, and (ii) identifying parameters which might be  
 156 uninfluential and whose values could be fixed (and excluded from a subsequent calibration  
 157 procedure) without affecting the model output (e.g., Hutcheson and McAdams, 2010; Liu et al.,  
 158 2006). We then perform our GSA after model parameters and weights are estimated through model  
 159 calibration against system state observations. At this stage, the main purpose of the GSA is that of  
 160 identifying parameters having the largest impact on the variation in the statistical moments of the  
 161 output, thus guiding additional efforts for their characterization.

162 The rest of the work is organized as follows. Section 2.1 describes the sensitivity  
 163 metrics/indices at core of the proposed GSA; Section 2.2 provides the expressions for multi-model  
 164 statistical moments of a target quantity; and Section 2.3 details the computational approach  
 165 employed. Section 3.1 and Section 3.2 exemplify the proposed methodology for the unconstrained  
 166 and constrained cases, respectively. A discussion is given in Section 4, and Section 5 provides our  
 167 major conclusions.

## 168 2. Methodology

### 169 2.1 Sensitivity Index

170 We consider a quantity  $\Delta$  (which represents a given modeling goal, e.g., concentration of  
 171 adsorbed metal onto soil or dissolved chemical in an aquifer, hydraulic head in a well, travel time of  
 172 a solute in a well-field, or other quantities of interest in an environmental scenario) that could be  
 173 rendered through a suite of  $N_M$  alternative (possibly competing) conceptual and mathematical  
 174 models collected in a model set  $\mathbf{M}$ . The latter somehow represents our ability to interpret a given  
 175 process or a set of processes contributing to characterize  $\Delta$ .

176 In the presence of observations of  $\Delta$ , one can rely on various criteria to (a) rank available  
 177 models, and/or (b) weigh results rendered by these models (e.g., Höge et al., 2019; Neuman, et al.  
 178 2012; Clark et al., 2008; Ye et al., 2008a, 2005, 2004; Poeter and Hill, 2007; Neuman et al., 2003).  
 179 In this context, one can evaluate prior (before new data/information about the system under analysis  
 180 become available (e.g., Rodríguez-Escales et al., 2018; Ye et al., 2008b) and posterior (after  
 181 data/information from the system are available (e.g., Bianchi Janetti et al., 2019, 2012; Ranee et al.,  
 182 2016; Moghadesi et al., 2015; Ye et al., 2008a) weights associated with each model included in  $\mathbf{M}$ .  
 183 Prior probability weights are usually taken to be equally apportioned amongst models or determined  
 184 on the basis of expert opinion. Posterior weights depend on the model discrimination criterion of  
 185 choice and on the prior weight associated with each model (e.g., Schöniger et al., 2014). Models  
 186 included in  $\mathbf{M}$  can be ranked according to such posterior weights or can be employed to provide  
 187 model-averaged statistics of the quantity of choice  $\Delta$ .

188 Each model  $M^j$  ( $j = 1, \dots, N_M$ ) in  $\mathbf{M}$  is characterized by a set of parameters, which we  
 189 collect in vector  $\theta^j$ . We treat each parameter of model  $j$ , i.e.,  $\theta_i^j$  ( $i = 1, \dots, N_j$ ) as a random  
 190 variable to account for our incomplete knowledge of its exact value. It is then possible to evaluate  
 191 the impact of uncertainties associated with both the models and their parameters on a quantity of  
 192 interest ( $\Delta$ ) in terms of moment-based sensitivity indices. We do so by extending the AMA  
 193 sensitivity indices introduced by Dell'Oca et al. (2017), that considered a unique system model with  
 194 uncertain parameters, to the case of possible multiple interpretative models, as rendered by the  
 195 collection of models included in  $\mathbf{M}$ .

196 Within this multi-model context, we quantify the sensitivity of a given statistical moment  
 197 (SM) to parameter  $\theta_i^j$  through the following index

$$198 \quad AMASM_{\theta_i^j} = \frac{w(M^j)}{\mathfrak{I}} \left\{ \underbrace{\left| SM[\Delta] - SM_{\theta^j}[\Delta | M^j] \right|}_{\text{model-choice contribution}} + E_{\theta_i^j} \left[ \underbrace{\left| SM_{\theta^j}[\Delta | M^j] - SM_{-\theta_i^j}[\Delta | M^j] \right|}_{\text{parameter-choice contribution}} \right] \right\} \quad (1)$$

199 with

$$200 \quad \mathfrak{S} = \begin{cases} |\text{SM}[\Delta]| & \text{if } \text{SM}[\Delta] \neq 0 \\ 1 & \text{if } \text{SM}[\Delta] = 0 \end{cases} \quad (2)$$

201 Here,  $AMASM_{\theta_i^j}$  is the *AMA* index associated with a given statistical moment  $\text{SM}$  (e.g.,  $\text{SM} = E$ ,  
202  $V$ ,  $\gamma$ ,  $k$  when considering the expected value, variance, skewness and kurtosis, respectively) of  $\Delta$   
203 considering the  $i$ -th parameter of model  $M^j$ ;  $w(M^j)$  is the (prior or posterior) probability of  
204 model  $M^j$ ;  $E_{\theta_i^j}$  is the expectation operator in the space of variability of  $\theta_i^j$ ;  $\text{SM}_{-\theta_i^j}[\Delta | M^j]$  and  
205  $\text{SM}_{\theta_i^j}[\Delta | M^j]$  correspond to the value of the statistical moment of  $\Delta$  considering uncertainty of  
206 (a) all parameters of model  $M^j$  except  $\theta_i^j$  (i.e., the value of the statistical moment resulting from  
207 conditioning to  $\theta_i^j$ ) and (b) the whole set of parameters in  $\theta^j$ , respectively. The quantity  $\text{SM}[\Delta]$   
208 in (1) represents the value of the given statistical moment of  $\Delta$  evaluated in a multi-model context,  
209 i.e., when both the model employed to interpret a given process and its associated parameters are  
210 uncertain. In Section 2.2 we provide further details about the evaluation of the statistical moment of  
211  $\Delta$  in a multi-model context. We note here that the first and the second terms in (1) are scalar  
212 quantities that can be consistently summed (see also discussion of Figure 1 below).

213 The rationale behind definition (1) is that the sensitivity of  $\Delta$ , as grounded on a set of  
214 statistical moments, to the parameter  $\theta_i^j$  is proportional to the induced variations of these statistical  
215 moments (with respect to their multi-model counterparts) due to the conditioning on the parameter  
216  $\theta_i^j$ . As such, the rationale at the core of (1) is different from that employed in GSA methodologies  
217 grounded on an uncertainty apportioning (e.g., Dai and Ye, 2015) or on a derivative based (e.g.,  
218 Razavi and Gupta, 2019; Rakovec et al. 2014, within the single-model context) rationales.

219 In the context of the proposed GSA, we emphasize that conditioning to  $\theta_i^j$  requires starting  
220 with selecting/choosing a model  $M^j$ . It then follows that two terms contribute to index  $AMASM_{\theta_i^j}$   
221 (1): (i) the first one is related to the choice of model  $M^j$  (within model vector  $\mathbf{M}$ ) and is termed  
222 here as the *model-choice contribution* (note that this contribution is common to all parameters in  
223  $M^j$  and is non-zero in the presence of multiple models, even if each model is characterized by  
224 deterministically known parameters); (ii) the second one is a *parameter-choice contribution* and  
225 represents the contribution to  $AMASM_{\theta_i^j}$  due to uncertainty of parameter  $\theta_i^j$  embedded in model  
226  $M^j$  (note that this contribution does not vanish in the presence of uncertain model parameters even  
227 in cases where there is only one available model; see also our discussion to Figure 1 below). It is  
228 also important to remark that indices  $AMASM_{\theta_i^j}$  are particularly suited for factor fixing studies  
229 because they allow highlighting those parameters that could potentially induce strong variations of  
230 the investigated statistical moments of the target model output.

231 Note that relying on multiple statistical moments explicitly recognizes that variance is not an  
232 exhaustive metric to quantify sensitivity (e.g., Dell’Oca et al., 2017; Pianosi and Wagner, 2015;  
233 Borgonovo, 2007; Liu et al., 2006).

234 Figure 1 depicts a sketch of the overall concept underpinning (1) when one considers two  
235 possible model choices,  $M^1$  and  $M^2$ , each associated with a set of two parameters, i.e.,  $(\theta_1^1, \theta_2^1)$   
236 for  $M^1$  and  $(\theta_1^2, \theta_2^2)$  for  $M^2$ . One can clearly visualize the nature of the diverse terms  
237 contributing to index  $AMASM_{\theta_i^j}$  through the depiction of Figure 1. Let us consider, for example,

238 index  $AMASM_{\theta_i^1}$ : (i) the distance between  $SM[\Delta]$  and  $SM_{\theta_i^1}[\Delta | M^1]$  (dark blue double pointed  
 239 arrow in Figure 1) corresponds to the model-choice contribution; (ii) the average (with respect to  
 240  $\theta_i^1$ ) distance between  $SM_{\theta_i^1}[\Delta | M_1]$  and  $SM_{-\theta_i^1}[\Delta | M^1]$  (light blue and blue double pointed  
 241 arrows for  $\theta_1^1$  and  $\theta_2^1$ , respectively) corresponds to the parameter-choice contribution for parameter  
 242  $\theta_i^1$  ( $i = 1, 2$ ); (iii) the sum of (i) and (ii), weighted by  $w(M^1)$  and normalized by  $SM[\Delta]$ , quantifies  
 243 the influence of  $\theta_i^1$  on  $\Delta$ , as expressed by index  $AMASM_{\theta_i^1}$ . The same line of reasoning can be  
 244 employed to describe the contributions of the parameters of  $M^2$  to our sensitivity indices. Note  
 245 that, in the presence of a unique interpretive model, e.g.,  $M^1$ , the distance between  $SM[\Delta]$  and  
 246  $SM_{\theta_i^1}[\Delta | M_1]$  vanishes, reflecting the deterministic choice of the model.

247 We recall here that when one considers only one interpretive model, the first term in (1)  
 248 vanishes and  $AMASM_{\theta_i^1}$  coincides with index  $AMASM_{\theta_i^1}$  defined by Dell’Oca et al. (2017), i.e.,

$$249 \quad AMASM_{\theta_i^1} \equiv AMASM_{\theta_i^1} = \frac{1}{\mathfrak{S}} E_{\theta_i^1} \left[ \left| SM_{\theta_i^1}[\Delta | M^j] - SM_{-\theta_i^1}[\Delta | M^j] \right| \right] \quad (3)$$

250 Comparison of (3) and (1) suggests that some similarities in the indices  $AMASM_{\theta_i^1}$  and  $AMASM_{\theta_i^1}$   
 251 are expected when the parameter-choice contribution in (1) is dominant.

## 252 **2.2 Multi-model Statistical Moments**

253 Here, we provide the details for the evaluation of the statistical moments of  $\Delta$  in a multi-  
 254 model context, i.e.,  $SM[\Delta]$ , leading to the evaluation of index (1). Introducing the probability  
 255 density function of  $\Delta$ ,  $p[\Delta]$ , as (e.g., Ye et al., 2004)

$$256 \quad p[\Delta] = \sum_{j=1}^{N_M} p[\Delta | M^j] w(M^j) \quad (4)$$

257 where  $p[\Delta | M^j]$  is the *pdf* of  $\Delta$  given model  $M^j$ , the expected value (first statistical moment) of  
 258  $\Delta$  is defined as

$$259 \quad E[\Delta] = \sum_{j=1}^{N_M} w(M^j) E_{\theta_i^1}[\Delta | M^j] \quad (5)$$

260 while the  $n$ -th order (central) moment can be evaluated as

$$261 \quad SM^{(n)}[\Delta] = \sum_{j=1}^{N_M} w(M^j) \sum_{k=0}^n \binom{n}{k} SM_{\theta_i^1}^{(k)}[\Delta | M^j] \left( E_{\theta_i^1}[\Delta | M^j] - E[\Delta] \right)^{n-k} \quad (6)$$

262 Variance,  $V = SM^{(2)}$ , skewness,  $\gamma = SM^{(3)} / V^{3/2}$  and kurtosis,  $k = SM^{(4)} / V^2$ , of  $\Delta$  can then be  
 263 assessed from (5) as

$$264 \quad V[\Delta] = \underbrace{\sum_{j=1}^{N_M} w(M^j) V_{\theta_i^1}[\Delta | M^j]}_{\text{within-model}} + \underbrace{\sum_{j=1}^{N_M} w(M^j) \left( E[\Delta] - E_{\theta_i^1}[\Delta | M^j] \right)^2}_{\text{between-model}} \quad (7)$$

265

266

$$\begin{aligned}
\gamma[\Delta] = & \sum_{j=1}^{N_M} \left( \frac{V_{\theta^j}[\Delta | M^j]}{V[\Delta]} \right)^{3/2} w(M^j) \gamma_{\theta^j}[\Delta | M^j] - \sum_{j=1}^{N_M} w(M^j) \frac{(E[\Delta] - E_{\theta^j}[\Delta | M^j])^3}{(V[\Delta])^{3/2}} \\
& \text{within-model} \qquad \qquad \qquad \text{between-model} \\
& - 3 \sum_{j=1}^{N_M} \frac{V_{\theta^j}[\Delta | M^j]}{(V[\Delta])^{3/2}} w(M^j) (E[\Delta] - E_{\theta^j}[\Delta | M^j]) \\
& \qquad \qquad \qquad \text{mixed}
\end{aligned} \tag{8}$$

268

$$\begin{aligned}
k[\Delta] = & \sum_{j=1}^{N_M} \left( \frac{V_{\theta^j}[\Delta | M^j]}{V[\Delta]} \right)^2 w(M^j) k_{\theta^j}[\Delta | M^j] + \sum_{j=1}^{N_M} w(M^j) \frac{(E[\Delta] - E_{\theta^j}[\Delta | M^j])^4}{(V[\Delta])^2} \\
& \text{within-model} \qquad \qquad \qquad \text{between-model} \\
& + 4 \sum_{j=1}^{N_M} w(M^j) \left( \frac{E[\Delta] - E_{\theta^j}[\Delta | M^j]}{V[\Delta]} \right)^2 \left\{ \frac{3}{2} V_{\theta^j}[\Delta | M^j] - \frac{\gamma_{\theta^j}[\Delta | M^j] (V_{\theta^j}[\Delta | M^j])^{3/2}}{E[\Delta] - E_{\theta^j}[\Delta | M^j]} \right\} \\
& \qquad \qquad \qquad \text{mixed}
\end{aligned} \tag{9}$$

270

271 The first term on the right hand side of (7) is typically referred to as the within-model variance and  
272 coincides with the average (across the collection of models) of the variances associated with each  
273 model whereas the second term in (7) is denoted as the between-model variance and is proportional  
274 to the *off-set* between  $E[\Delta]$  and  $E_{\theta^j}[\Delta | M^j]$  (e.g., Draper, 1995). Along the same line, one  
275 recognizes that equations (8)-(9) show that, in a multi-model context, the shape of the distribution  
276 of  $\Delta$ , as quantified by skewness and kurtosis, is affected by the following three terms: (i) a within-  
277 model component, which corresponds to the weighted average of the values (of skewness or  
278 kurtosis) rendered by each model, the weights being proportional to  $w(M^j)$  and the ratio between  
279  $V_{\theta^j}[\Delta | M^j]$  and  $V[\Delta]$ ; (ii) a between-model component, which is proportional to the *off-set*  
280  $(E[\Delta] - E_{\theta^j}[\Delta | M^j])$ ; and (iii) a mixed component, that takes into account the *off-set*  
281  $(E[\Delta] - E_{\theta^j}[\Delta | M^j])$  (i.e., the between-model variability) as well as the variability within each  
282 model, as quantified by  $V_{\theta^j}[\Delta | M^j]$  in (7) or by  $V_{\theta^j}[\Delta | M^j]$  and  $\gamma_{\theta^j}[\Delta | M^j]$  in (8).

283 It is here important to note that (a) our definition of sensitivity in (1) is grounded on the  
284 assessment of the (average) variation of a SM due to conditioning on a given parameter in a given  
285 model while (b) formulations (7)-(9) serve uncertainty apportioning, i.e., (7)-(9) allow identifying  
286 the main factors (between model format and model parameters) contributing to the uncertainty of an  
287 output of interest.

288

### 2.3 Numerical Evaluation

289 Inspection of equation (1) reveals that one needs to evaluate  $SM_{-\theta^j}[\Delta | M^j]$ , i.e., the  
290 statistical moment of  $\Delta$  conditional to diverse values of  $\theta_i^j$ , considering model  $M^j$ . Here, we do  
291 so through a straightforward Monte Carlo sampling scheme. We (i) discretize the support of each  
292 parameter by way of a given number of equal bins, i.e.,  $N_{bins}$  (for simplicity we employ the same



293 value of  $N_{bins}$  for all parameters) and (ii) evaluate the conditional statistical moment,  
 294  $SM_{-\theta_i^j} [\Delta | M^j]$ , associated with each bin. We then proceed to evaluate the second term in (1) by  
 295 taking expectation with respect to  $\theta_i^j$ , i.e.,  $E_{\theta_i^j}$ . The unconditional statistical moment, i.e.,  
 296  $SM_{\theta^j} [\Delta | M^j]$ , is evaluated through the algebraic expressions (4)-(8). Convergence of the results  
 297 with respect to the  $N_{bins}$  is assessed by increased the latter by regular increments of 10 until the  
 298 relative variation of all investigated quantities is smaller than a fixed threshold. Here, for simplicity  
 299 and ease of implementation we select the median value within each bin as representative and  
 300 evaluate each model under investigation considering all of the combinations of the parameter values  
 301 identified according to this, i.e., we run model  $j$  for a total of  $(N_{bins})^{N_j}$  times. As such, while more  
 302 efficient sampling strategies can be employed, there are no particular constraints in the sampling  
 303 scheme one can employ in our GSA.

### 304 3. Illustrative examples

305 As a showcase example to illustrate the application of the theoretical framework introduced in  
 306 Section 2, we focus on the geochemical process of sorption of metals onto soil matrices. We do so  
 307 by leveraging on the study of Bianchi Janetti et al. (2012) who analyze the ability of diverse  
 308 isotherm models to interpret experimental observations documenting copper sorption onto Bet  
 309 Dagan soil type (see Table 1 of Bianchi Janetti et al. (2012) for the description of the key  
 310 characteristics of the soil type). For each experiment, 1g of soil was mixed with 40 mL of a solution  
 311 containing copper. Seven diverse initial concentrations were considered. The same initial pH was set  
 312 for all experiments. The resulting mixture was then shaken for 48 h to attain equilibrium. A 10-mL  
 313 sample of the solution was then extracted and passed through a 0.22  $\mu\text{m}$  filter. Copper concentration  
 314 was evaluated by inductively coupled plasma-mass spectrometry. Three replicates were performed  
 315 for each initial concentration, the resulting average and variance (assumed to represent  
 316 measurement error variance) being employed in the calibration procedure. The complete description  
 317 of the details of the experimental set-up and conditions are offered by Bianchi Janetti et al. (2012).

318 The following three commonly used interpretive isotherm models have been considered by  
 319 Bianchi Janetti et al. (2012) to interpret the experimental results,

$$320 \quad c_0 = \frac{K^F c^{n^F}}{V} + c \quad \text{Freundlich (F)} \quad (10a)$$

$$321 \quad c_0 = \frac{1}{V} \frac{q_m^L K^L c}{1 + K^L c} + c \quad \text{Langmuir (L)} \quad (10b)$$

$$322 \quad c_0 = \frac{1}{V} \frac{K^R c}{1 + \alpha^R c^{\beta^R}} + c \quad \text{Redlich-Peterson (R)} \quad (10c)$$

323 Here,  $c_0$  ( $\text{mmol L}^{-1}$ ) and  $c$  ( $\text{mmol L}^{-1}$ ) are the concentration of solute initially dissolved in the fluid  
 324 and adsorbed onto the soil, respectively;  $V$  ( $\text{L g}^{-1}$ ) is the ratio between the solution volume and the  
 325 soil mass considered in the batch experiments. The Freundlich model (Freundlich, 1906) is based on  
 326 the assumption that sorption energies are characterized by an exponential distribution. The model is  
 327 parameterized by the partition coefficient  $K^F$  ( $\text{L}^{n^F} \text{mmol}^{1-n^F} \text{g}^{-1}$ ) and a dimensionless exponent  $0 <$   
 328  $n^F < 1$ . The Langmuir model (Langmuir, 1918) assumes that sorption takes place at a fixed  
 329 number of well-localized sites, all of which are characterized by uniformly distributed sorption  
 330 energies, whereas  $q_m^L$  ( $\text{mmol g}^{-1}$ ) corresponds to the saturation of all sorption sites and  $K^L$  ( $\text{L}$   
 331  $\text{mmol}^{-1}$ ) is the adsorption rate. The Redlich-Peterson model (Redlich-Peterson, 1959) is a  
 332 combination of the Freundlich and Langmuir models is parameterized by  $K^R$  ( $\text{L g}^{-1}$ ),  $\alpha^R$  ( $\text{L g}^{-1}$ )

333  $L^{\beta^R} \text{mmol}^{-\beta^R}$ ) and  $0 < \beta^R < 1$ . We follow Bianchi Janetti et al. (2012) and present our results in  
 334 terms of mass per volume of solute, i.e.,  $C$  ( $\text{mg L}^{-1}$ ).

335 In the following we focus on to two diverse cases: unconstrained (Section 3.1; i.e., no data are  
 336 employed to constrain model parameters and weights) and constrained (Section 3.2; i.e., model  
 337 parameters and weights are evaluated on the basis of the experimental results).

### 338 3.1 Unconstrained case

339 Here, we perform the (moment-based) global sensitivity analysis detailed in Section 2 by  
 340 considering the statistical moment of  $C$  before the parameters and weights of the candidate models  
 341 are constrained through calibration against available observations. We term this case as  
 342 unconstrained. In this context, we assign an equal weight,  $w(M^j) = 1/3$ , to each of the models

343 (10a)-(10c). We treat parameter uncertainties by assuming model parameters  $\theta_i^j$  as independent  
 344 identically distributed (iid) random variables, characterized by a uniform probability density  
 345 function (reflecting the lack of prior knowledge about model parameters) and a constant coefficient  
 346 of variation,  $CV_{\theta_i^j}$  (to reduce biases in the analysis arising from considering diverse relative

347 intervals of variation for each  $\theta_i^j$ ). Note that our proposed GSA approach is not limited to the  
 348 specific choices we consider in this study, whereas the use of diverse formats of the prior  
 349 distribution of  $\theta_i^j$  and of diverse values of  $CV_{\theta_i^j}$  are fully compatible with the approach. We set

350  $CV_{\theta_i^j} = 0.7$ , to consider a relatively wide parameter space defined as

351  $\left[1 - \sqrt{3}CV_{\theta_i^j}, 1 + \sqrt{3}CV_{\theta_i^j}\right] \times E[\theta_i^j]$ ,  $E[\theta_i^j]$  being the expected value of  $\theta_i^j$  listed in Table 1,

352 taken to coincide with the corresponding parameter estimate evaluated by Bianchi Janetti et al.  
 353 (2012). Regarding the convergence of the results, we verified that that considering  $N_{bins} = 100$  (i.e.,  
 354  $10^4$  or  $10^6$  evaluations of the Freundlich and Langmuir models or the Redlich-Peterson model,  
 355 respectively) was sufficient to ensure a relative variation smaller than 1% for all of the considered  
 356 results.

357 Figure 2 depicts the (a) expected value,  $E_{\theta^j}[C|M^j]$ , (b) variance,  $V_{\theta^j}[C|M^j]$ , (c)  
 358 skewness,  $\gamma_{\theta^j}[C|M^j]$ , and (d) kurtosis  $k_{\theta^j}[C|M^j]$ , of the adsorbed concentration  $C$  versus the  
 359 initial solute concentration,  $C_0$ , conditional to the Freundlich (black curve), the Langmuir (blue  
 360 curves) or the Redlich-Peterson (red curves) model. The corresponding multi-model statistical  
 361 moments are also depicted (purple curves). For all statistical moments of order larger than one we  
 362 also depict the within-model (dashed purple curves) and the between-model (dotted purple curves)  
 363 contributions. Figures 2c-d also include the mixed terms (dash-dotted curves, see definition in (8)-  
 364 (9)).

365 Overall inspection of Figure 2 shows that in each model all statistical moments (hence the  
 366 shape of the *pdf*) of  $C$  depends on  $C_0$ . All centered SMs (see Figure 2b-d) are well approximated  
 367 by their within-model contributions, the between-model contribution for the variance being at least  
 368 an order of magnitude smaller than the within-model terms, and the between-model and mixed  
 369 terms for skewness and kurtosis being close to zero. As such, the uncertainty about the model (as  
 370 imbued in the variability of the center of mass of the *pdfs* of  $C$ ) to describe the adsorbed  
 371 concentrations has a minor role on the ensuing uncertainty in  $C$  (as rendered through the centered  
 372 SMs here analyzed) than our lack of knowledge about the model parameters.

373 Figure 3a depicts indices  $AMA E_{K^F}$  (black continuous curve) and  $AMA E_{n^F}$  (blue curve)  
 374 together with the corresponding model-choice (red continuous curve) and parameter-choice

375 (symbols) contributions as a function of  $C_0$ . These results are complemented by Figure 3b,  
 376 depicting indices  $AMAE_{K^F}$  (black curve) and  $AMAE_{n^F}$  (blue curve), which are obtained by  
 377 assuming that the Freundlich isotherm is associated with a unit weight (i.e., corresponding to a  
 378 single model approach). Figures 3c, d and Figures 3e, f show the corresponding results performed  
 379 for the Langmuir and Redlich-Peterson models, respectively.

380 Joint inspection of Figures 3a, c, e reveals that the parameter-choice contributions (linked to  
 381 parameter variability given a selected model) practically coincide with indices  $AMAE_{\theta_j}$ , the model-  
 382 choice contribution being at least one order of magnitude smaller than the parameter-choice  
 383 contribution. Comparison of indices  $AMAE_{K^F}$  and  $AMAE_{n^F}$  in Figure 3a reveals that the influence  
 384 of  $K^F$  on the expected value of  $C$  is larger than that of  $n^F$  for all values of  $C_0$ . This suggests that  
 385 the uncertainty of  $K^F$  has, on average, a stronger impact than that of  $n^F$  on the mean of  $C$ . Figure  
 386 3c shows that  $K^L$  influences the expected value of  $C$  to a greater extent than  $q_m^L$  for low  $C_0$ ,  
 387 these two parameters tending to be equally influential as  $C_0$  increases. Figure 3e shows that  
 388 indices  $AMAE_{\alpha^R}$  and  $AMAE_{\beta^R}$  are significantly smaller than  $AMAE_{K^R}$  and all three indices  
 389 decrease with increasing  $C_0$ . One can also note that index  $AMAE_{\theta_j}$  (Figure 3a, c, e) and its  
 390 counterpart  $AMAE_{\theta_i}$  (Figures 3b, d, f) display a similar trend when plotted versus  $C_0$ . This result  
 391 suggests that for this unconstrained setting (where each model is associated with the same weight)  
 392 the uncertainty in the model parameters induces very similar contributions to the relative change of  
 393 the expected value of  $C$ , regardless of whether one relies on a multi- or a single-model approach.

394 Similar results have been obtained for indices  $AMAV_{\theta_j}$  (see Figure 4),  $AMAY_{\theta_j}$  (see Figure  
 395 A.1) and  $AMAK_{\theta_j}$  (see Figure A.2).

### 396 3.2 Constrained case

397 Here, we perform our GSA after adsorption data become available and model parameters and  
 398 weights are estimated by means of model calibration. We term this as constrained case and diagnose  
 399 the influence of the residual (i.e., following model calibration) uncertainty associated with model  
 400 parameters on the statistical moments of  $C$  in the presence of various models.

401 We rely on the model calibration results of Bianchi Janetti et al. (2012) who estimate model  
 402 parameters through a Maximum Likelihood (ML) (see e.g., Carrera and Neuman, 1986) procedure  
 403 and (posterior) model weights  $w(M_j)$  on the bases of the Kashyap (1982) model discrimination  
 404 criterion (KIC), allowing to consider (i) measurement error variance in the parameter estimation  
 405 process as well as (ii) conceptual model uncertainty (see e.g., Höge et al., 2019; Moghadasi et al.,  
 406 2015; Bianchi Janetti et al., 2012; Ye et al., 2004). Parameter estimates and posterior weights are  
 407 listed in Table 1. Consistent with the ML procedure adopted for model calibration, a Gaussian  
 408 density is associated with each model parameter, which is then characterized by its (estimated)  
 409 mean and standard deviation.

410 All our results are based on  $N_{bins} = 100$ , a value that is consistent with the unconstrained case  
 411 and is sufficient to ensure a relative variation smaller than 1% for all of the considered results.

412  
 413 Table 1. Results of the ML model calibrations (from Bianchi Janetti et al. (2012)).

Model	Parameter	Estimated Mean Value	Standard Deviation	Coefficient of Variation	Model weight
Freundlich	$K^F$	0.99	0.04	0.04	0.8851

(10a)	$n^F$	0.26	0.05	0.19	
Langmuir	$K^L$	0.28	0.41	1.46	
(10b)	$q_m^L$	2.86	0.09	0.03	0.0369
Redlich-	$K^R$	3.89	0.14	0.04	
Peterson	$\alpha^R$	3.28	0.16	0.05	0.0780
(10c)	$\beta^R$	0.79	0.01	0.01	

414

415 Figure 5 is the counterpart of Figure 2 based on the ML model calibration results and  
 416 posterior model weights of Table 1. Figure 5a also includes the experimental data (black dots).

417 A striking feature of Figure 5a is the marked/modest relative differences observed for  
 418 low/high  $C_0$  between the expected values of  $C$  resulting from the diverse interpretive models  
 419 considered. Note that such relative differences tend to be larger/smaller than those recorded for the  
 420 unconstrained case (see Figure 2a) for the lowest/largest values of  $C_0$ . These features are  
 421 consistent with the observation that only few data are available for model calibration at low  $C_0$ .

422 Comparison of  $V_{\theta^j}[C|M^j]$  and  $V[C]$  in Figure 5b and in Figure 2b reveals that both  
 423 quantities are smaller for the constrained than for the unconstrained scenario, with the exception of  
 424  $V_{\theta^L}[C|M^L]$ . This result is consistent with the reduced relative uncertainty (as expressed through  
 425 the coefficient of variation) associated with the parameter values estimated through model  
 426 calibration (with the exception of  $CV_{K^L}$ ) with respect to their prior (or unconstrained) counterparts  
 427 (for which  $CV_{\theta^j}=0.7$ ). We further note that in the constrained case the between-model  
 428 contribution to  $V[C]$  can be of the same order of magnitude of (or even larger than) the  
 429 corresponding within-model contribution. The latter result is a consequence of model calibration  
 430 that causes a redistribution of the relative importance of the lack of knowledge about (a) model  
 431 parameters and (b) model structure on the variability of  $C$ .

432 The comparison of  $\gamma_{\theta^j}[C|M^j]$  in Figure 5c and in Figure 2c reveals a reduction of the  
 433 skewness of the *pdfs* of  $C$  as rendered by the Freundlich and Redlich-Peterson models (  
 434  $\gamma_{\theta^F}[C|M^F]$  and  $\gamma_{\theta^R}[C|M^R]$  almost vanished in the constrained scenario), and an increase of  
 435  $\gamma_{\theta^L}[C|M^L]$  for the constrained respect to the unconstrained scenario. On the other hand,  $\gamma[C]$   
 436 (purple curve) is significantly larger ( $\sim$  one order of magnitude) in the constrained than in the  
 437 unconstrained scenario. Figure 5c also indicates that the within-model contributions (dashed purple  
 438 curve) are dominant to  $\gamma[C]$ , followed by the mixed term (dot-dashed purple curve). The major  
 439 factor causing the dominance of the within-model contribution (see the first term in (8)) is the term  
 440 associated with the Langmuir model which, despite having a low model weight (= 0.0369), exhibits  
 441 a high ratio between  $V_{\theta^L}[C|M^L]$  and  $V[C]$ . This observation is sustained by the observed  
 442 similarity in the trend of  $\gamma_{\theta^L}[C|M^L]$  and  $\gamma[C]$ , as a function of  $C_0$ . A similar behavior emerges  
 443 also from the comparison of  $k_{\theta^j}[C|M^j]$  and  $k[C]$  (see Figure 5d and Figure 2d), and is again due  
 444 to the dominance of the factor associated with the Langmuir model in the within-model contribution  
 445 in (9).

446 Comparison of the sensitivity indices in Figure 6 with their counterparts in Figure 3 provides  
 447 an indication of the way the influence of each model parameter on the expected value of  $C$ , as  
 448 expressed in terms of  $AMAE_{\theta_j}$ , evolves as information about the system under investigation are  
 449 acquired. It is possible to note that (a) the parameter-choice contributions to  $AMAE_{\theta_j}$  in Figures 6a,  
 450 c, e are smaller than in the uniformed case (Figure 3a, c, e), as a consequence of the model  
 451 calibration procedure (with exception of the term associated with  $K^L$ ); and (b) the model-choice  
 452 contribution increases and becomes dominant for most of the parameters for low  $C_0$ , in agreement  
 453 with the previously noted marked relative discrepancies between the  $E_{\theta_j} [C | M_j]$  for the three  
 454 considered models (see Figure 5). Results included in Figure 7 complement those of Figure 4 for  
 455 the constrained case. Comparison of these two sets of results clearly indicates that, following data  
 456 acquisition, the major factor contributing to each index  $AMAV_{\theta_j}$  tends to be the model-choice  
 457 contribution rather than the component associated with the parameter-choice contributions, a sole  
 458 exception being given by  $AMAV_{K^L}$ . Inspection of sensitivity indices grounded on the skewness,  
 459  $AMAY_{\theta_j}$  (Figure A.3), and the kurtosis,  $AMAK_{\theta_j}$  (Figure A.4), provides results in line with those  
 460 for the expected value and the variance (see Appendix A).

461 Comparison of  $AMASM_{\theta_j}$  (Figure 6-7a, c, e) and their counterparts  $AMASM_{\theta_i}$  (Figure 6-  
 462 7b, d, f) reveals that for the constrained case the influence of  $i$ -th parameter on the mean and  
 463 variance of  $C$  could either change markedly (when the model-choice contribution is the dominant  
 464 one) or only marginally (when the parameter-choice contribution is dominant) as a consequence of  
 465 considering only one or multiple models. These aspects are encapsulated, for example, in the results  
 466 depicting the behavior of (i) the Freundlich and Redlich-Peterson models, where the model-choice  
 467 contribution to  $AMAV_{\theta_j}$  is the most relevant component, or (ii) the results for  $K^L$  in the Langmuir  
 468 model, where the parameter-choice contribution to  $AMAV_{K^L}$  is the dominant term. Similar results  
 469 are detected for the sensitivity indices grounded on the skewness and the kurtosis of the *pdfs* of  $C$   
 470 (see Appendix A).

#### 471 4. Discussion

472 The comparison of the importance of the model-choice and parameter-choice contributions  
 473 for the unconstrained and constrained cases highlights that: (a) in the former case, where all models  
 474 are associated with equal weight, the influence of the choice of the model on the statistical moments  
 475 of  $C$  are negligible with respect to the impact of the uncertainty of the model parameters; (b) in the  
 476 latter case, the variability of the first four statistical moments of  $C$  is more strongly controlled by the  
 477 residual lack of knowledge about the adequacy of each of the candidate models to interpret the  
 478 system rather than by the residual uncertainty about the estimated model parameters; (c) an  
 479 exception to the observed decreased influence of the parameter-choice contributions is noted with  
 480 reference to  $K^L$ , whereas the quality of the estimate of this parameter is quite modest (i.e., the  
 481 corresponding coefficient of variation is higher than that considered for the unconstrained case, see  
 482 Table 1), thus leading to a strong sensitivity of the SMs of  $C$  to  $K^L$  even as the Langmuir model is  
 483 associated with a low posterior model weight. From a practical perspective, these observations  
 484 suggest that the variability in the SMs of  $C$  here analyzed could be further constrained by: (i)  
 485 collecting additional data with the aim of reducing uncertainty associated with estimates of  $K^L$  or  
 486 (ii) excluding the Langmuir model from model set  $\mathbf{M}$ , in light of its low model weight.

487 We note that the results could be impacted by considering diverse formats of the *pdfs* of the  
 488 parameters either in the unconstrained or in the constrained case (whereas we rely on a uniform and  
 489 Gaussian distribution, respectively). Diverse studies, performed in a single-model context, highlight

490 the relevance of the choice of the parameters' distributions on the results of a GSA (e.g., Paleari and  
491 Confalonieri, 2016; Shin et al., 2013; Wang et al., 2013; Kelleher et al., 2011). Furthermore, it has  
492 to be recognized that the results of the GSA here performed could also depend on the method  
493 employed to estimate model weights (here we resort to the Kashyap (1982) model discrimination  
494 criterion (KIC), as described in Section 3.2). It would then be of interest to analyze in future studies  
495 the relevance of diverse choices for these elements within the context of multi-model GSAs.

496 For the sake of clarity in the interpretation of the results, we recall here that (a) the sensitivity  
497 index in (1) corresponds to the (average) variation of a SM due to conditioning on a given  
498 parameter in a given model while (b) formulations (7)-(9) allow quantifying the contribution to the  
499 uncertainty of an output stemming from the model format and parameters. Thus, it is not surprising  
500 that, for the constrained case here examined, even as the behavior of the multi-model skewness and  
501 kurtosis of  $C$  (see Figure 5) (and, to a lesser extent, that of the multi-model variance) are clearly  
502 dictated by the terms associated with the Langmuir model in the within-model contributions in (8)-  
503 (9), it is yet possible that the major contributing factor to the sensitivity index for a parameter (e.g.,  
504  $\beta^R$  or  $q_m^L$ ) is the model-choice contribution.

505 From a physical perspective, the results for the unconstrained case suggest an overall major  
506 relevance of parameter  $K^j$  (with  $j = F, L, R$ ) on the modeling goals. While this parameter is  
507 associated with a different specific meaning depending on the model, it can be generally understood  
508 as a constant of proportionality driving the intensity of the sorption process. As mentioned in  
509 Section 1, we focus on the unconstrained case to gain insight about model functioning, and it is in  
510 such a set-up that we can mitigate possible bias about parameter relevance associated with diverse  
511 relative sizes of the *pdfs*' supports (i.e., we impose the same coefficient of variation for each  
512 parameter) and with diverse model weights (i.e., each model has the same weight). Otherwise,  
513 results for the constrained case are more suited to guide further system investigations.

514 With reference to the numerical sampling scheme, we point out that the formulation in (1)  
515 does not prevent the use of other, and possibly more efficient, sampling strategies, as compared to  
516 the one we detail in Section 2.3. We further note that considering complex and computationally  
517 expensive models might require reducing the computational burden by leveraging on the use of a  
518 surrogate model, given the ability of the latter to successfully render the required statistical  
519 moments (see e.g., Dell'Oca et al. 2017).

520 As a final remark, we note that it could be of interest to evaluate the way a (statistical)  
521 moment of  $\Delta$  is influenced by (a) a parameter (synthesizing some properties/features of the  
522 investigated system) in cases where the latter appears in more than one model in  $\mathbf{M}$ ; or (b) diverse  
523 conceptualizations and/or mathematical formulations of the various processes embedded in a model  
524 of the system under investigation. These aspects might assist in exploring answers to questions of  
525 the kind 'to which processes are the statistical moments of  $\Delta$  most sensitive? Is such a sensitivity  
526 due to the uncertainty about process conceptualization or is it mainly due to parametric uncertainty  
527 employed in our conceptualization of each process?'. We present the mathematical formulation  
528 associated with these aspects in Appendix B and C, respectively. Comparisons of the present  
529 methodology with other multi-model GSAs (e.g., Dai et al., 2017; Dai and Ye, 2015) will be the  
530 subject of future studies, where we will consider the case where parameters appear in more than one  
531 model in  $\mathbf{M}$  (in the showcase introduced in Section 3 each of the parameters considered was  
532 associated with a unique model), as well as the possibility that a model comprises processes for  
533 which alternative conceptualizations are available (here, we consider a unique process, i.e.,  
534 adsorption).

## 535 5. Conclusions

536 Our work leads to the following major findings.

- 537 1) We develop and illustrate sensitivity indices providing metrics for global sensitivity  
538 across multiple interpretive models with uncertain parameters. We assess the sensitivity  
539 of the first four statistical moments of a target quantity of interest ( $\Delta$ ) with respect to its

- 540 variations related to the uncertainty in the model structure and associated parameters.  
541 Our illustrative example demonstrates that a given parameter can be associated with  
542 diverse degrees of importance, depending on the statistical moment of  $\Delta$  considered.
- 543 2) Our (moment-based) sensitivity indices are structured according to two key components:  
544 (a) a model-choice contribution, which takes into account the possibility of analyzing the  
545 system of interest by taking advantage of various model conceptualizations (or  
546 mathematical renderings); (b) a parameter-choice contribution, associated with the  
547 uncertainty in the parameters of a selected model.
  - 548 3) In the showcase example analyzed, involving three competing models to interpret  
549 concentration of metal sorption on soil samples,  $C$ , the values of the proposed sensitivity  
550 indices vary depending on whether we diagnose the system response prior to acquiring  
551 data on  $C$  or after observing the outcomes of some experiments and performing  
552 Maximum Likelihood models calibration with ensuing estimation of probability weights  
553 related to each model. Our moment-based indices resulting from the latter setting (here  
554 termed as constrained scenario) quantify the influence of the residual (i.e., following  
555 model calibration) uncertainty associated with model parameters on the statistical  
556 moments of  $C$  in the presence of multiple models.
  - 557 4) Our results show that in the absence of conditioning on observations of  $C$  (here termed  
558 as unconstrained scenario) all sensitivity indices are dominated by the variability in the  
559 model parameters, contributions due to the various model conceptualizations being at  
560 least of an order of magnitude smaller. Otherwise, conditioning on acquired  $C$  data  
561 yields a decrease in the values of the sensitivity indices (a symptom of reduced relative  
562 variability in the ensuing statistical moments of  $C$ ) and an increases of the model-choice  
563 contribution that could be of the same order of magnitude of (or even greater than) the  
564 parameter-choice term. An exception to the latter observation is noted for indices  
565 associated with parameters which estimates are characterized by poor quality.

#### 566 **Acknowledgements**

567 The authors are grateful to the EU and MIUR for funding, in the frame of the collaborative  
568 international Consortium (WE-NEED) financed under the ERA-NET WaterWorks2014 Cofunded  
569 Call. This ERA-NET is an integral part of the 2015 Joint Activities developed by the Water  
570 Challenges for a Changing World Joint Programme Initiative (Water JPI). Prof. A. Guadagnini  
571 acknowledges funding from Région Grand-Est and Strasbourg-Eurométropole through the ‘Chair  
572 Gutenberg’. Data are available online (<http://dx.doi.org/10.17632/55nmwbfpg.1>).

#### 574 **References**

- 575 Baroni, G., & Tarantola, S. (2014). A general probabilistic framework for uncertainty and global  
576 sensitivity analysis of deterministic models: A hydrological case study. *Environmental*  
577 *Modelling & Software*, 51, 26-34.
- 578 Beven, K. (2006). A manifesto for the equifinality thesis. *Journal of Hydrology*, 320, 18-36.
- 579 Bianchi Janetti, E., Dror, I., Riva, M., Guadagnini, A., & Berkowitz, B. (2012). Estimation of  
580 single-metal & competitive sorption isotherms through Maximum Likelihood and Model Quality  
581 Criteria. *Soil Science Society American Journal*, 76(4). 1229-1245. doi:10.2136/sssaj2012.0010.
- 582  
583 Bianchi Janetti, E., Guadagnini, L., Riva, M., & Guadagnini, A. (2019). Global sensitivity analyses  
584 of multiple conceptual models with uncertain parameters driving groundwater flow in a regional-  
585 scale sedimentary aquifer. *Journal of Hydrology*, 574, 544-556. doi:  
586 10.1016/j.jhydrol.2019.04.035.  
587

- 588 Bredehoeft, J. D. (2005). The conceptualization model problem-surprise. *Hydrogeology Journal*,  
589 13, 37-46.  
590
- 591 Borgonovo, E., & Plischke, E. (2016). Sensitivity Analysis: a review of recent advances. *European*  
592 *Journal of Operational Research*, 248, 869-887. doi:10.1016/j.ejor.2015.06.032.
- 593 Borgonovo, E. (2007). A new uncertainty importance measure. *Reliability Engineering System*  
594 *Safety*, 92, 771-784.
- 595 Burnham, K. P., & Anderson, A. R. (2002). Model Selection and Multiple Model Inference: A  
596 Practical Information-Theoretical Approach. 2<sup>nd</sup> ed., *Springer*, New York.  
597
- 598 Carrera, J., & Neuman, S. P. (1986). Estimation of aquifer parameters under transient and steady  
599 state conditions: 1. Maximum likelihood method incorporating prior information. *Water*  
600 *Resources Research*, 22 (2), 199-210.  
601
- 602 Chu, J., Zhang, C., Fu, G., Li, Y., & Zhou, H. (2015). Improving multi-objective reservoir operation  
603 optimization with sensitivity constrained dimension reduction. *Hydrology Earth System Science*,  
604 19, 3557-3570. doi.org/10.5194/hess-19-3557-2015.  
605
- 606 Ciriello, V., Edery, Y., Guadagnini, A., & Berkowitz, B. (2015). Multimodel framework for  
607 characterization of transport in porous media. *Water Resources Research*, 51(5), 3384-3402.  
608 doi:10.1002/2015WR017047.  
609
- 610 Clark, M. P., Slater, A. G., Rupp, D. E., Woods, R. A., Vrugt, J. A., Gupta, H. V., Wagner, T., &  
611 Hay, L. E. (2008). Framework for Understanding Structural Errors (FUSE): A modular  
612 framework to diagnose differences between hydrological models. *Water Resources Research*,  
613 44(12). <https://doi.org/10.1029/2007WR006735>.  
614
- 615 Dai, H., & M. Ye (2015). Variance-based global sensitivity analysis for multiple scenarios and  
616 models with implementation using sparse grid collocation. *Journal of Hydrology*, 528, 286-300.  
617 doi:10.1016/j.jhydrol.2015.06.034.
- 618 Dai, H., Ye, M., Walker, A. P., & Chen, X. (2017). A new process sensitivity index to identify  
619 important system processes under process model and parametric uncertainty. *Water Resources*  
620 *Research*, 53, 3476–3490. doi:10.1002/2016WR019715.  
621
- 622 Degenring, D., Froemel, C., Dikta, G., & Takors, R. (2004). Sensitivity analysis for the reduction of  
623 complex metabolism models. *Journal of Process Control*, 14(7), 729-745.
- 624 Dell’Oca, A., Riva, M., & Guadagnini, A. (2017). Moment-based metrics for global sensitivity  
625 analysis of hydrological systems. *Hydrology Earth System Science*, 21, 6219-6234.  
626 doi:10.5194/hess-21-6219-2017.  
627
- 628 Draper, D. (1995). Assessment and propagation of model uncertainty. *Journal of the Royal*  
629 *Statistical Society, Series B*, 57(1), 45-97.  
630
- 631 Fajraoui, N., Ramasomanana, F., Younes, A., Mara, T.A., Ackerer, P., & Guadagnini, A. (2011).  
632 Use of Global Sensitivity Analysis and Polynomial Chaos Expansion for Interpretation of Non-  
633 reactive Transport Experiments in Laboratory-Scale Porous Media. *Water Resources Research*,  
634 47, W02521. doi:10.1029/2010WR009639.  
635



- 636 Förster, K., Meon, G., Marke, T., & Strasser, U. (2014). Effect of meteorological forcing & snow  
637 model complexity on hydrological simulations in the Sieber catchment (Harz Mountains,  
638 Germany). *Hydrology Earth System Science*, 18, 4703-4720. doi:10.5194/hess-18-4703-2014.  
639
- 640 Gupta, H. V., Wagener, T., & Liu, Y. Q. (2008). Reconciling theory with observations: Elements of  
641 a diagnostic approach to model evaluation. *Hydrology Processes*, 22(18), 3802–3813.
- 642 Gupta, H. V., & Razavi, S. (2018). Revisiting the basis of sensitivity analysis for dynamical earth  
643 system models, *Water Resources Research*, 54(11), 8692-8717.  
644 <https://doi.org/10.1029/2018WR022668>.
- 645 Hill, M. C., Foglia, L., Christensen, S., Rakovec, O., & Borgonovo, E. (2016). Model validation:  
646 Testing models using data and sensitivity analysis. *The Handbook of Groundwater Engineering*,  
647 edited by Cushman J. H. & Tartakovsky, D., 3rd ed., Taylor & Francis, Boca Raton, Fla.  
648 doi:10.1201/9781315371801-22.  
649
- 650 Herman, J. D., Kollat, J. B., Reed, P. M., & Wagener, T. (2013). From maps to movies: high-  
651 resolution time-varying sensitivity analysis for spatially distributed watershed models.  
652 *Hydrology Earth System Science*, 17, 5109–5125. doi:10.5194/hess-17-5109-2013.  
653
- 654 Höge, M., Wöhling, T., & Nowak, W. (2018). A primer for model selection: the decisive role of  
655 model complexity. *Water Resources Research*, 54(3), 1688-1715. doi:10.1002/2017WR021902.  
656
- 657 Höge, M., Guthke, A., & Nowak, W. (2019). The hydrologist's guide to Bayesian model selection,  
658 averaging and combination. *Journal of Hydrology*, 572, 96-107.  
659 <https://doi.org/10.1016/j.jhydrol.2019.01.072>.
- 660
- 661 Hölter, R., Zhao, C., Mahmoudia, E., Lavasan, A. A., Datcheva, M., Königa, M., & Schanza, T.  
662 (2018). Optimal measurements design for parameter identification in mechanized tunneling.  
663 *Underground Space*, 3(1), 34-44. doi:10.1016/j.undsp.2018.01.004.  
664
- 665 Hutcheson, R. S., & McAdams, D. A. (2010). A hybrid sensitivity analysis for use in early design.  
666 *Journal of Mechanical Design*, 132(11). doi:10.1115/1.4001408.  
667
- 668 Kashyap, R. L. (1982). Optimal choice of AR and MA parts in autoregressive moving average  
669 models. *IEEE Transaction on Pattern Analysis and Machine Intelligence*, 4(2), 99–104.  
670
- 671 Kass, R. E., & Raftery, A. E. (1995). Bayes factors. *Journal of the American statistical association*,  
672 90(430), 773-795.  
673
- 674 Kelleher, C., Wagener, T., Gooseff, M., McGlynn, B., McGuire, K. & Marshall, L. (2012).  
675 Investigating controls on the thermal sensitivity of Pennsylvania streams. *Hydrological*  
676 *Processes*, 26, 771-785. doi:10.1002/hyp.8186.  
677
- 678 Knuth, K. H., Habeck, M., Malakar, N. K., Mubeen, A. M., & Placek, B. (2015). Bayesian evidence  
679 and model selection. *Digital Signal Processes*, 47, 50–67.  
680
- 681 Koutsoyiannis, D. (2010). HESS Opinions “A random walk on water”. *Hydrology Earth System*  
682 *Science*, 14, 585-601. doi:10.5194/hess-14-585-2010.  
683
- 684 Liu, H., Sudjianto, A., & Chen, W. (2006). Relative entropy based method for probabilistic  
685 sensitivity analysis in engineering design. *Journal of Mechanical Design*, 128, 326-336.

686  
687  
688  
689  
690  
691  
692  
693  
694  
695  
696  
697  
698  
699  
700  
701  
702  
703  
704  
705  
706  
707  
708  
709  
710  
711  
712  
713  
714  
715  
716  
717  
718  
719  
720  
721  
722  
723  
724  
725  
726  
727  
728  
729  
730  
731  
732  
733  
734  
735

Liu, P., Elshall, A. S., Ye, M., Beerli, P., Zeng, X., Lu, D., & Tao, Y. (2016). Evaluating marginal likelihood with thermodynamic integration method and comparison with several other numerical methods. *Water Resources Research*, 52, 734–758. doi:10.1002/2014WR016718.

Moghadasli, L., Guadagnini, A., Inzoli, F., & Bartosek, M. (2015). Interpretation of two-phase relative permeability curves through multiple formulations and model quality criteria. *Journal of Petroleum Science Engineering*, 126, 738-749. doi:10.1016/j.petrol.2015.10.027.

Muleta, M. K., & Nicklow, J. W. (2005). Sensitivity and uncertainty analysis coupled with automatic calibration for a distributed watershed model. *Journal of Hydrology*, 306, 127-145.

Neuman, S. P. (2003). Maximum likelihood Bayesian averaging of alternative conceptual-mathematical models. *Stochastic Environmental Research and Risk Assessment*, 17 (5), 291-305. doi:10.1007/s00477-003-0151-7.

Neuman, S.P., Xue, L., Ye, M., & Lu, D. (2012). Bayesian analysis of data-worth considering model and parameter uncertainties. *Advances in Water Research*, 36, 75-85. doi:10.1016/j.advwatres.2011.02.007.

Nossent, J., Elsen, P., & Bauwens, W. (2011). Sobol' sensitivity analysis of a complex environmental model. *Environmental Modelling Software*, 26(12), 1515–1525.

Paleari, L., & Confalonieri, R. (2016). Sensitivity analysis of a sensitivity analysis: We are likely overlooking the impact of distributional assumptions. *Ecological Modelling*, 340, 57–63. <https://doi.org/10.1016/j.ecolmodel.2016.09.008>.

Paniconi, C., & Putti, M. (2015). Physically based modeling in catchment hydrology at 50: survey and outlook. *Water Resources Research*, 51, 7090–7129. doi:10.1002/2015WR017780.

Pappenberger, F., Beven, K. J., Ratto, M., & Matgen, P. (2008). Multi-method global sensitivity analysis of flood inundation models. *Advances Water Research*, 31(1), 1–14.

Pianosi, F., Beven, K., Freer, J., Hall, J. W., Rougier, J., Stephenson, D. B., & Wagener, T. (2016). Sensitivity analysis of environmental models: A systematic review with practical workflow. *Environmental Modelling & Software*, 79, 214-232.

Pianosi, F., & Wagener, T. (2015). A simple and efficient method for global sensitivity analysis based on cumulative distribution functions. *Environmental Modelling & Software*, 67, 1-11.

Poeter, E. P., & Anderson, D. A. (2005). Multimodel ranking and inference in ground water modeling. *Ground Water*, 43 (4), 597–605.

Poeter, E. P., & Hill, M. C. (2007). MMA: A computer code for multi-model analysis. *United States Geological Survey, Technology & Methods 6-E3*, USGS, Reston, Va.

Punzo, V., Marcello, M., & Biagio, C. (2015). Do we really need to calibrate all the parameters? Variance-based sensitivity analysis to simplify microscopic traffic flow models. *IEEE Transaction on Intelligent Transport Systems*, 16, 184-193.

- 736 Rakovec, O., Hill, M. C., Clark, M., Weerts, A., Teuling, A., & Uijlenhoet, R. (2014). Distributed  
737 evaluation of local sensitivity analysis (DELSA), with application to hydrologic models. *Water*  
738 *Resources Research*, 50(1), 409-426. <https://doi.org/10.1002/2013WR014063>.  
739
- 740 Ranaee, E., Riva, M., Porta, G., & Guadagnini, A. (2016). Comparative Assessment of Three-  
741 Phase Oil Relative Permeability Models. *Water Resources Research*, 52, 1-16.  
742 doi:10.1002/2016WR018872.  
743
- 744 Razavi, S., & Gupta, H. V. (2019). A multi-method generalized global sensitivity matrix approach  
745 to accounting for the dynamical nature of earth and environmental systems. *Environmental*  
746 *Modelling & Software*, 114, 1-11. <https://doi.org/10.1016/j.envsoft.2018.12.002>.  
747
- 748 Razavi, S., & Gupta, H. V. (2016a). A new framework for comprehensive, robust, and efficient  
749 global sensitivity analysis: Part I – Theory. *Water Resources Research*, 52, 423-439.  
750 doi:10.1002/2015WR017558.  
751
- 752 Razavi, S., & Gupta, H. V. (2016b). A new framework for comprehensive, robust, and efficient  
753 global sensitivity analysis: Part II – Applications. *Water Resources Research*, 52, 440-455.  
754 doi:10.1002/2015WR017559.  
755
- 756 Rodríguez-Escales, P., Canelles, A., Sanchez-Vila, S., Folch, A., Kurtzman, D., Rossetto, R.,  
757 Fernández-Escalante, E., Lobo-Ferreira, J.-P., Sapiano, M., San-Sebastián, J., & Schüth, C.  
758 (2018). A risk assessment methodology to evaluate the risk failure of managed aquifer recharge  
759 in the Mediterranean Basin. *Hydrology Earth System Science*, 22, 3213-3227. doi:10.5194/hess-  
760 22-3213-2018.  
761
- 762 Ruano, M. V., Ribes, J., Seco, A., & Ferrer, J. (2012). An improved sampling strategy based on  
763 trajectory design for application of the Morris method to systems with many input factors.  
764 *Environmental Modelling & Software*, 37, 103–109.  
765
- 766 Saltelli, A., Ratto, M., Andres, T., Campolongo, F., Cariboni, J., Gatelli, D., Saisana, M., &  
767 Tarantola, S. (2008). Global Sensitivity Analysis. The Primer, Wiley, 305 pp.  
768
- 769 Schoniger, A., Wholing, T., Samaniego, L., & Nowak, W. (2014). Model selection on solid ground:  
770 rigorous comparison of nine ways to evaluate Bayesian model Evidence. *Water Resources*  
771 *Research*, 50. doi:10.1002/2014WR016062.  
772
- 773 Schoups, G., & Hopmans, J. W. (2006). Evaluation of model complexity and input uncertainty of  
774 field-scale water flow and transport. *Vadose Zone Journal*, 5, 951-962.  
775 doi:10.2136/vzj2005.0130.  
776
- 777 Shin, M. J., Guillaume, J. H. A., Croke, B. F. W., & Jakeman, A. J. (2013). Addressing ten  
778 questions about conceptual rainfall-runoff models with global sensitivity analyses. *Journal of*  
779 *Hydrology*, 503, 135-152. <https://doi.org/10.1016/j.jhydrol.2013.08.047>.  
780
- 781 van Griensven, A., Meixner, T., Grunwald, S., Bishop, T., Diluzio, M., & Srinivasan, R. (2006). A  
782 global sensitivity analysis tool for the parameters of multi-variable catchment models. *Journal of*  
783 *Hydrology*, 324(1–4), 10–23.  
784

785 Wagener, T., van Werkhoven, K., Reed, P., & Tang, Y. (2009). Multiobjective sensitivity analysis  
786 to understand the information content in streamflow observations for distributed watershed  
787 modeling. *Water Resources Research*, 45, W02501. doi:10.1029/2008WR007347.  
788

789 Wagener, T., & Montanari, A. (2011). Convergence of approaches toward reducing uncertainty in  
790 predictions in ungauged basins. *Water Resources Research*, 47, W060301.  
791 doi:10.1029/2010WR009469, 2011.  
792

793 Wang, S., Ancell, B. C., Huang, G. H., & Baetz, B. W. (2018). Improving Robustness of  
794 Hydrologic Ensemble Predictions Through Probabilistic Pre- & Post-Processing in Sequential  
795 Data Assimilation. *Water Resources Research*, 54(3). 2129-2151. doi:10.1002/2018WR022546.  
796

797 Wang, J., Li, X., Lu, L., & Fang, F. (2013). Parameter sensitivity analysis of crop growth models  
798 based on the extended Fourier Amplitude Sensitivity Test method. *Environmental Modelling and  
799 Software*, 48, 171-182. <https://doi.org/10.1016/j.envsoft.2013.06.007>.  
800

801 Wöhling, T., & Vrugt, J. A. (2008). Combining multiobjective optimization & Bayesian model  
802 averaging to calibrate forecast ensembles of soil hydraulic models. *Water Resources Research*,  
803 44, W12432. doi:10.1029/2008WR007154.  
804

805 Younes, A., Delay, F., Fajraoui, N., Fahs, M., & Mara, T. A. (2016). Global sensitivity analysis and  
806 Bayesian parameter inference for solute transport in porous media colonized by biofilms. *Journal  
807 of Contaminant Hydrology*, 191, 1-18. doi:10.1016/j.jconhyd.2016.04.007.  
808

809 Ye, M., Neuman, S. P., & Meyer, P. D. (2004). Maximum likelihood Bayesian averaging of spatial  
810 variability models in unsaturated fractured tuff. *Water Resources Research* 40, W05113.  
811 doi.org/10.1029/2003WR002557.  
812

813 Ye, M., Neuman, S. P., Meyer, P. D., & Pohlmann, K. F. (2005). Sensitivity analysis and  
814 assessment of prior model probabilities in MLBMA with application to unsaturated fractured  
815 tuff. *Water Resources Research*, 41, W12429. doi:10.1029/2005WR004260.  
816

817 Ye, M., Meyer, P. D., & Neuman, S. P. (2008). On model selection criteria in multimodel analysis.  
818 *Water Resources Research*, 44, W03428. doi:10.1029/2008WR006803.  
819

820 Ye, M., Pohlmann, K. F., & Chapman, J. B. (2008). Expert elicitation of recharge model  
821 probabilities for the Death Valley regional flow system. *Journal of Hydrology*, 354, 102-115.  
822

823 Yue, H., Brown, M., He, F., Jia, J., & Kell, D. B. (2008). Sensitivity analysis & robust  
824 experimental design of a signal transduction pathway system. *International Journal of Chemical  
825 Kinetics*, 40, 730-741. doi:10.1002/kin.20369.  
826

827 **Appendix A. Sensitivity Analysis grounded on the Skewness and the Kurtosis of model output,**  
828 **Unconstrained and Constrained Scenarios.**

829 Figure A.1a depicts  $AMA\gamma_{K^F}$  (black continuous curve) and  $AMA\gamma_{n^F}$  (blue curve) together  
830 with the corresponding model-choice (red continuous curve) and parameter-choice (symbols)  
831 contributions as a function of  $C_0$  for the unconstrained scenario. These results are complemented  
832 by Figure A.1b, depicting indices  $AMA\gamma_{K^F}$  (black curve) and  $AMAE_{n^F}$  (blue curve), which are  
833 obtained by assuming a unit weight (i.e., single model approach) for the Freundlich isotherm (10a).  
834 Figures A.1c-A.1d and Figures A.1e-f show the corresponding results obtained for the Langmuir  
835 (10b) and Redlich-Peterson (10c) models, respectively. Figure A.2 depicts the collection of  
836 companion results for  $AMAK_{\theta^j}$  and  $AMAK_{\theta_i}$ .

837 Joint analysis of Figures A.1-A.2 and Figures 2-3 reveals an overall similarity in the  
838 sensitivity of the first four statistical moments of  $C$  with respect to (i) the parameters of each model,  
839 either in the multi- or single-model context, and (ii) the (less relevant) contributions associated with  
840 the model choice.

841 Figures A.3-A.4 are the counterparts of Figures A.1-A.2 for the constrained scenario,  
842 respectively. Comparison of Figures 3.A - 4.A with Figures 6 - 7 indicates an overall similarity of  
843 the sensitivity of the diverse SMs with respect to parameters- and the model-choice contributions.  
844

845 **Appendix B. Extension of the AMA sensitivity indices for the multi-model context when a**  
846 **parameter appears within multiple models.**

847 One can assess the influence that a parameter associated with multiple models can have on a  
848 given statistical moment (SM) of an investigated quantity ( $\Delta$ ) in terms of the following indices  
849

$$850 \quad AMASM_{\theta_i^M} = \sum_{M^j: \theta_i \in \theta^j} AMASM_{\theta_i^j} \quad (B.1)$$

851 where  $AMASM_{\theta_i^j}$  is given by (1). The key difference between  $AMASM_{\theta_i^j}$  and  $AMASM_{\theta_i^M}$  is that  
852 the former answers the question ‘how does the variability in a given parameter influence  $SM[\Delta]$ ,  
853 when we look at such a parameter only in model  $M^j$ ?’ while the latter answers the question ‘how  
854 does the variability in a given parameter influence  $SM[\Delta]$ , when we look at such a parameter  
855 across the set of models within which it appears?’.

856 As such, index  $AMASM_{\theta_i^j}$  allows quantifying the implications on SM of selecting model  $M^j$   
857 (at the expenses of other models) and setting parameter  $\theta_i^j$  to a given value. Otherwise,  
858  $AMASM_{\theta_i^M}$  focuses on the diagnosis of the relevance of parameter  $\theta_i$  across a collection of  
859 competing model alternatives within which  $\theta_i$  appears. Note that  $AMASM_{\theta_i^M} \equiv AMASM_{\theta_i^j}$  if  $\theta_i$  is  
860 associated with only one model of the collection.

861 When  $SM[\Delta]$  corresponds to the variance of  $\Delta$ , it should be noted that  $AMAV_{\theta_i}$  differs from  
862 the index  $S_{\theta_i}$  proposed by Dai and Ye (2015) and defined as

$$S_{\theta_i} = \frac{\sum_{M^j: \theta_i^j \subseteq \theta^j} w(M^j) \left( E_{\theta_i^j} \left[ V_{\theta^j} [\Delta | M^j] - V_{-\theta_i^j} [\Delta | M^j] \right] \right)}{\sum_{M^j: \theta_i^j \subseteq \theta^j} w(M^j) V_{\theta^j} [\Delta | M^j]} \quad (2.B)$$

Index  $S_{\theta_i}$  quantifies the influence of  $\theta_i^j$  to  $\Delta$  as the ratio between: (i) the expected change of the variance of  $\Delta$  for a given model, i.e.,  $V_{\theta^j} [\Delta | M^j]$ , due to the knowledge of parameter  $\theta_i^j$ , as averaged over all of the models in which  $\theta_i^j$  appears; and (ii) the weighted-average (over the diverse competing models in which  $\theta_i^j$  appears) of  $V_{\theta^j} [\Delta | M^j]$ . As such,  $AMAV_{\theta_i}$  and  $S_{\theta_i}$  convey different information about the nature of the sensitivity of  $\Delta$  with respect to  $\theta_i^j$ .

With reference to the showcase detailed in Section 3, it should be noted that index  $S_{\theta_i}$  in (2.B) coincides with the well-known Sobol index, given that each parameter  $\theta_i^j$  appears only in a given model  $M^j$  and not across a set of models.

### Appendix C. Embedding uncertainty of model processes within the AMA indices

The metric proposed in Section 2 (Eq. (1)) could be modified to evaluate the sensitivity of a given statistical moment with respect to the possibility of rendering a process (or multiple processes) involved in the model construction through a variety of alternative mathematical formulations. In this context, each model,  $M^j$  in the set  $\mathbf{M}$  is viewed as a union of diverse processes, i.e.,

$$M^j = \left( \cup P^k (\theta^{j,k}) \right) \quad (C.1)$$

Here,  $P^k$  is the  $k$ -th process and  $\theta^{j,k}$  is the vector of parameters relevant to the  $k$ -th process, as rendered through the mathematical formulation associated with model  $M^j$ . As an example, a subsurface solute transport model of an adsorbable compound could include a variety of processes (e.g., adsorption, advection, hydrodynamic dispersion, distributed recharge, or others), each characterized by its own set of parameters. All possible combinations of the identified model processes give rise to the set of models  $\mathbf{M}$ .

It is then possible to group such  $k$  mathematical formulations of a given process within vector  $\mathbf{P}^k$ . One can quantify the influence of these various mathematical formulations of the process on a target statistical moment (SM) of an investigated quantity ( $\Delta$ ) as

$$AMASM_{P^k} = \frac{1}{\mathfrak{S}} \sum_{M^j: P^k \subseteq \mathbf{P}^k | M^j} w(M^j) \left\{ \left[ \text{SM}[\Delta] - \text{SM}_{\theta^{j,k}, -P^k} [\Delta | M^j] \right] \right\} +$$

*model-choice contribution*

$$+ \frac{1}{\mathfrak{S}} \sum_{M^j: P^k \subseteq \mathbf{P}^k | M^j} w(M^j) \left\{ \sum_{\theta_i^{j,k} | M^j} E_{\theta_i^{j,k} | M^j} \left[ \left[ \text{SM}_{\theta^{j,k}, -P^k} [\Delta | M^j] - \text{SM}_{-\theta_i^{j,k}, -P^k} [\Delta | M^j] \right] \right] \right\}$$

*parameter-choice contribution*

(C.2)

Here,  $\text{SM}_{\theta^{j,k}, -P^k} [\Delta | M^j]$  is the selected statistic, which is evaluated considering variability in the parameters of the  $k$ -th process in model  $M^j$ , the variability associated with other processes components, i.e.,  $-P^k$ , having been averaged out;  $\text{SM}_{-\theta_i^{j,k}, -P^k} [\Delta | M^j]$  is the statistic conditioned to parameter  $\theta_i^{j,k}$ , of process  $P^k$  and given  $M^j$ , the variability associated with the remaining

895 parameters of  $P^k$  given  $M^j$  having been averaged out (as well as the one linked to other  
 896 processes, i.e.,  $-P^k$ , in model  $M^j$ ).

897 Note that it is still possible to distinguish between (a) a contribution due to variability in the  
 898 conceptualization (or mathematical rendering) of a process and (b) a contribution determined by the  
 899 lack of knowledge about the parameters appearing in the mathematical formulation of the process.  
 900 The former or the latter contribution vanishes if the mathematical model of the  $k$ -th process or its  
 901 parameters are deterministically known, respectively.

902 Figure D.1 depicts a sketch of the overall concept underpinning index  $AMASM_{P^k}$  when only  
 903 two processes (i.e.,  $k = 1, 2$ ) are considered. Three conceptualizations of process  $P^1$  are considered,  
 904 each characterized by two parameters affected by uncertainty. Otherwise, only one  
 905 conceptualization is considered for process  $P^2$ , whose parameters are taken to be deterministic.  
 906 This gives rise to three distinct models. Note that values of  $SM_{\theta^{j,k}, -P^k} [\Delta | M^j]$  for  $k = (1, 2)$   
 907 coincide in this example, because  $P^2$  is deterministically known.

908 One can then visualize the nature of the various contributions to index  $AMASM_{P^k}$  through  
 909 the depiction of Figure C.1. When considering, for example, index  $AMASM_{P^1}$ , we observe that: (i)  
 910 the sum of the distances between  $SM[\Delta]$  and  $SM_{\theta^{j,1}, -P^1} [\Delta | M^j]$  (dark purple double pointed  
 911 arrow) across models  $M^j$  corresponds to the model-choice contribution; (ii) the weighted sum over  
 912 the models  $M^j$  of the averaged distances between  $SM_{\theta^{j,1}, -P^1} [\Delta | M^j]$  and  $SM_{-\theta_i^{j,1}, -P^1} [\Delta | M^j]$   
 913 (dark and light blue, green and yellow double pointed arrows for parameters  $\theta_1^{j,1}$  and  $\theta_2^{j,1}$  in model  
 914  $M^1$ ,  $M^2$ , and  $M^3$ , respectively) corresponds to the parameter-choice contribution. We remark  
 915 that, even as we consider only one conceptualization (here with deterministic parameter(s)) for  
 916 process  $P^2$ , there is still a model-choice contribution (as quantified by the black double pointed  
 917 arrows in Figure 1.C) which reflects the observation that  $\Delta$  is determined by the interaction of  
 918 processes  $P^1$  and  $P^2$ .

919 In case  $SM[\Delta]$  corresponds to the variance of  $\Delta$  (i.e.,  $SM[\Delta] \equiv V[\Delta]$ ), it should be noted  
 920 that  $AMASM_{P^k}$  differs from the index  $S_{P^k}$  proposed by Dai *et al.* [2017], which reads

$$921 \quad PS_k = \sum_{M^j: P^k \subseteq P^k | M^j} \frac{w(M^j) \{V[\Delta] - V_{\theta^{j,k}, -P^k} [\Delta | M^j]\}}{V[\Delta]} \quad (C.3)$$

922  
 923 The latter identifies the most influential process as the one leading to the highest reduction of  
 924 the overall variance of  $\Delta$ . As such, it is a metric focusing on apportionment of uncertainty (due to  
 925 variability in model process conceptualization). Otherwise, index  $AMASM_{P^k}$  is keyed to  
 926 quantifying variability in a given statistical moment of  $\Delta$ , highlighting the contribution due to  
 927 uncertainty in the process conceptualization and in the process parameter(s). It is then clear that  
 928  $AMASM_{P^k}$  and  $PS_k$  provide different information and could potentially be jointly used to assist  
 929 comprehensive sensitivity analyses, a topic which is the subject of a future study.

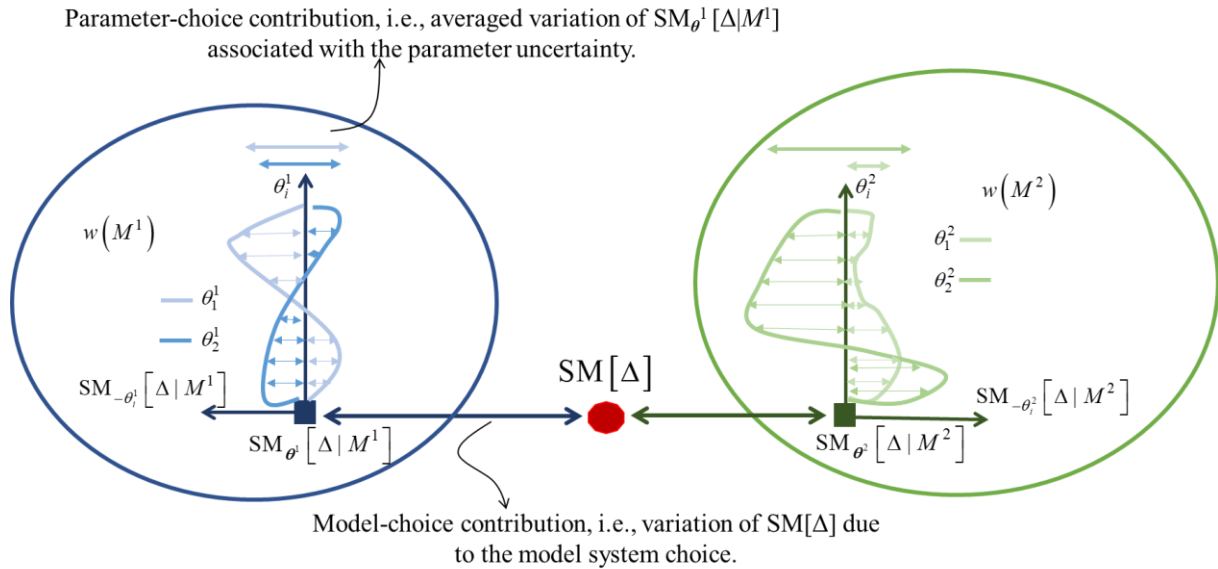
930           With reference to the showcase detailed in Section 3, the evaluation of (C.2) and (C.3) would  
931 be of very limited interest, given that each model  $M^j$  encompasses only one process (i.e.,  
932 adsorption).  
933



934

Figures

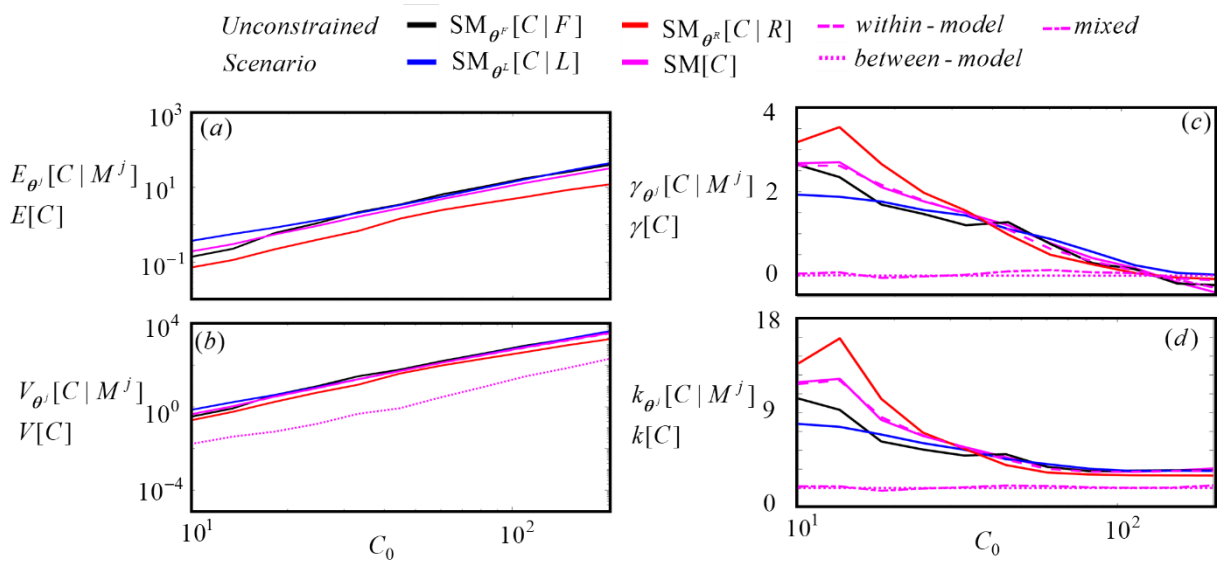
935



936

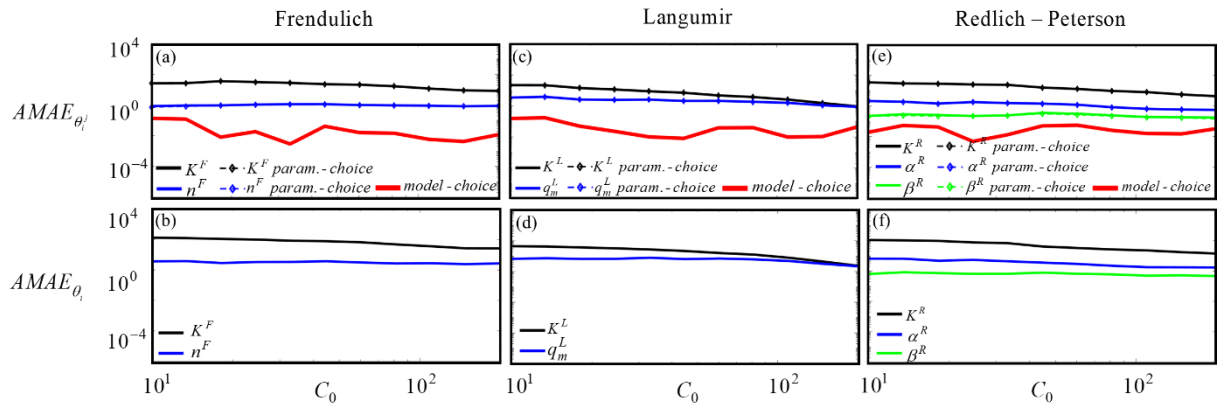
937 **Figure 1.** Sketch of the overall concept underpinning the sensitivity indices in (1), considering the  
 938 generic statistical moment  $SM$  for the quantity of interest  $\Delta$ . For ease of illustration we consider  
 939 only two interpretative models,  $M^1$  and  $M^2$ , with corresponding model weights  $w(M^1)$  and  $w(M^2)$   
 940 ). Each model has a set of two uncertain parameters, i.e.,  $(\theta_1^1, \theta_2^1)$  for  $M_1$  and  $(\theta_1^2, \theta_2^2)$  for  $M_2$ .  
 941  $SM[\Delta]$ ,  $SM_{\theta^i}[\Delta|M^j]$  and  $SM_{\cdot\theta^i}[\Delta|M^j]$  with  $j=(1, 2)$  and  $i=(1, 2)$  correspond to the  
 942 ensuing  $SM$  evaluated in a multi-model context, evaluated considering uncertainty in all the  
 943 parameters of model  $M^j$  and evaluated considering uncertainty in all the parameters of model  $M^j$   
 944 except  $\theta_i^j$ .

945



946  
947  
948  
949  
950  
951  
952  
953  
954  
955  
956  
957  
958  
959  
960  
961  
962  
963  
964  
965  
966  
967  
968  
969

**Figure 2.** Unconstrained scenario, a) expected value, (b) variance, (c) skewness, and (d) kurtosis, of the adsorbed concentration  $C$  versus the initial solute concentration,  $C_0$ , conditional to the Freundlich (black curve), the Langmuir (blue curves) and the Redlich-Peterson (red curves) model. The corresponding multi-model statistical moments are also depicted (purple curves). For all central statistical moments the within-model (dashed purple curves) and the between-model (dotted purple) contributions are also depicted. Figures 2c-d also include the mixed terms (defined in (7)-(8)).



970

971

972

973

974

975

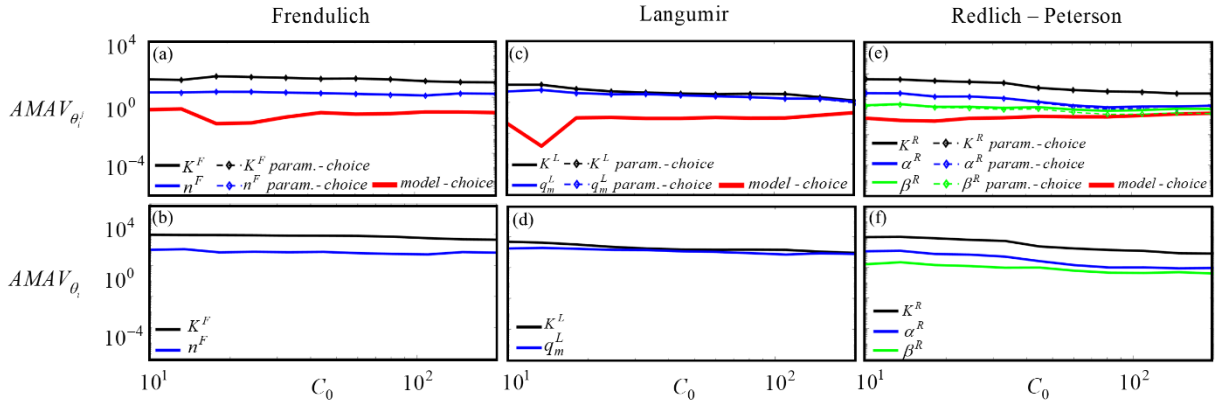
976

977

978

979

**Figure 3.** Unconstrained scenario. Sensitivity indices (1) associated with the expected value of  $C$  for the multi-model context versus  $C_0$  considering (a) the Freundlich ( $AMA E_{K^F}$ , black continuous curve, and  $AMA E_{n^F}$ , blue continuous curve); (c) the Langumir ( $AMA E_{K^L}$ , black continuous curve, and  $AMA E_{q_m^L}$ , blue continuous curve); (e) the Redlich-Peterson ( $AMA E_{K^R}$ , black continuous curve,  $AMA E_{\alpha^R}$ , blue continuous curve, and  $AMA E_{\beta^R}$ , green continuous curve). For each index the corresponding (i) parameter-choice contribution (symbols) and (ii) the model-choice contribution (red curves) are also depicted. The counterparts for the single-model context are depicted for (b) the Freundlich, (d) the Langumir and (f) the Redlich-Peterson model.



981

982

983

984

985

986

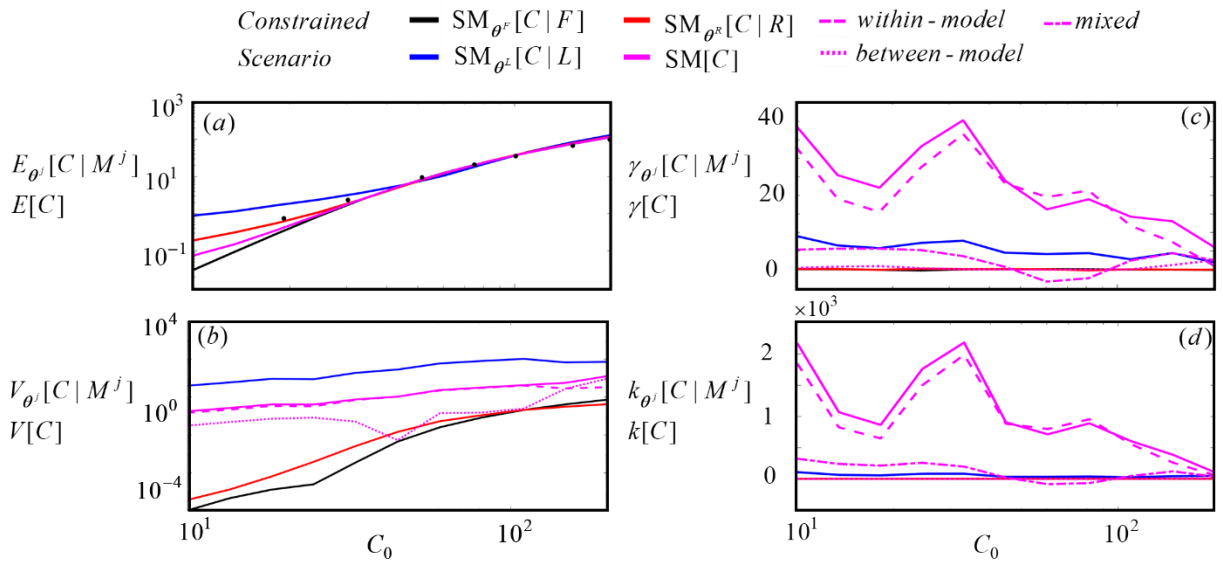
987

988

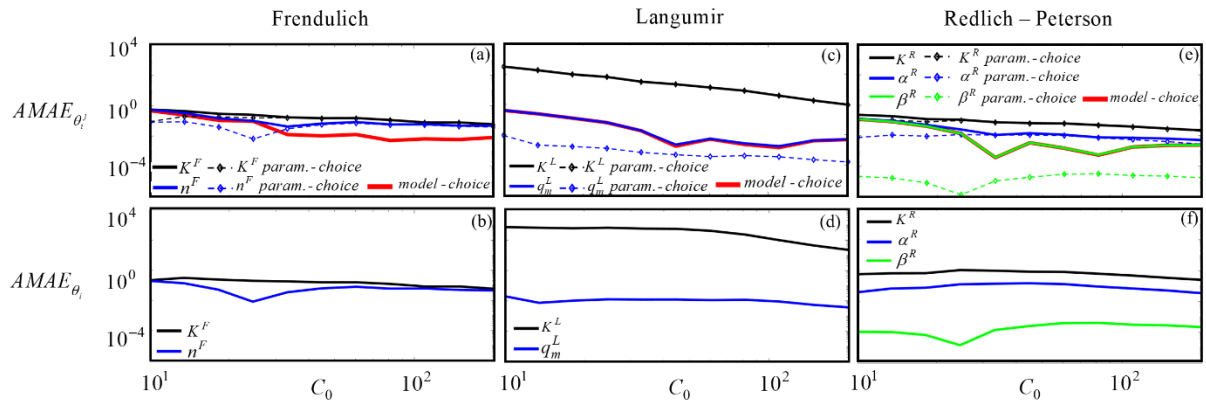
989

990

**Figure 4.** Unconstrained scenario. Sensitivity indices (1) associated with the Variance of  $C$  for the multi-model context versus  $C_0$  considering (a) the Freundlich ( $AMA E_{K^F}$ , black continuous curve, and  $AMA E_{n^F}$ , blue continuous curve); (c) the Langumir ( $AMA E_{K^L}$ , black continuous curve, and  $AMA E_{q_m^L}$ , blue continuous curve); (e) the Redlich-Peterson ( $AMA E_{K^R}$ , black continuous curve,  $AMA E_{\alpha^R}$ , blue continuous curve, and  $AMA E_{\beta^R}$ , green continuous curve). For each index the corresponding (i) parameter-choice contribution (symbols) and (ii) the model-choice contribution (red curves) are also depicted. The counterparts for the single-model context are depicted for (b) the Freundlich, (d) the Langumir and (f) the Redlich-Peterson model.



991  
 992 **Figure 5.** Constrained scenario, (a) expected value, (b) variance, (c) skewness, and (d) kurtosis, of  
 993 the adsorbed concentration  $C$  versus the initial solute concentration,  $C_0$ , conditional to the  
 994 Freundlich (black curve), the Langmuir (blue curves) and the Redlich-Peterson (red curves) model.  
 995 The corresponding multi-model statistical moments are also depicted (purple curves). For all central  
 996 statistical moments the within-model (dashed purple curves) and the between-model (dotted purple)  
 997 contributions are also depicted. Figures 5c-d also include the mixed terms (defined in (7)-(8)).  
 998  
 999  
 1000  
 1001  
 1002  
 1003  
 1004  
 1005  
 1006  
 1007  
 1008  
 1009  
 1010  
 1011  
 1012  
 1013  
 1014



1015

1016

1017

1018

1019

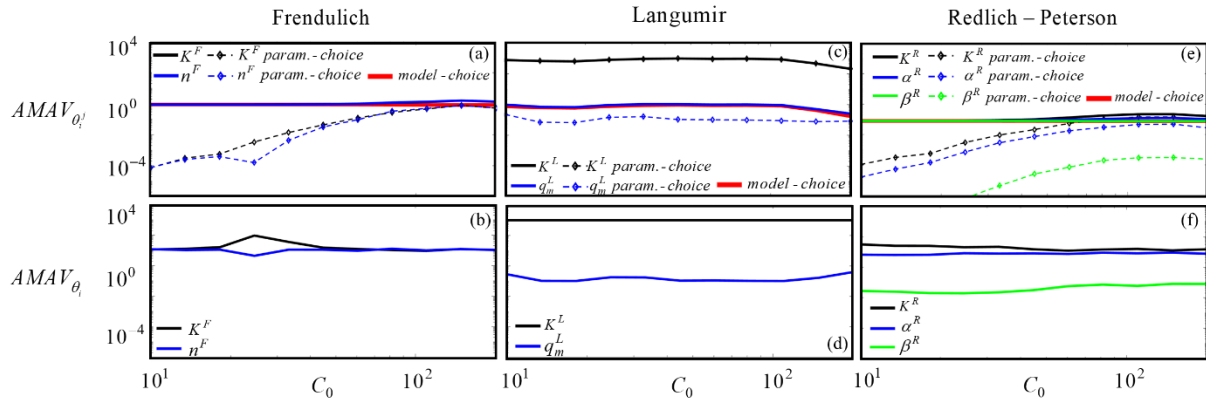
1020

1021

1022

1023

**Figure 6.** Constrained scenario. Sensitivity indices (1) associated with the expected value of  $C$  for the multi-model context versus  $C_0$  considering (a) the Freundlich ( $AMA E_{K^F}$ , black continuous curve, and  $AMA E_{n^F}$ , blue continuous curve); (c) the Langumir ( $AMA E_{K^L}$ , black continuous curve, and  $AMA E_{q_m^L}$ , blue continuous curve); (e) the Redlich-Peterson ( $AMA E_{K^R}$ , black continuous curve,  $AMA E_{\alpha^R}$ , blue continuous curve, and  $AMA E_{\beta^R}$ , green continuous curve). For each index the corresponding (i) parameter-choice contribution (symbols) and (ii) the model-choice contribution (red curves) are also depicted. The counterparts for the single-model context are depicted for (b) the Freundlich, (d) the Langumir and (f) the Redlich-Peterson model.



1025

1026

1027

1028

1029

1030

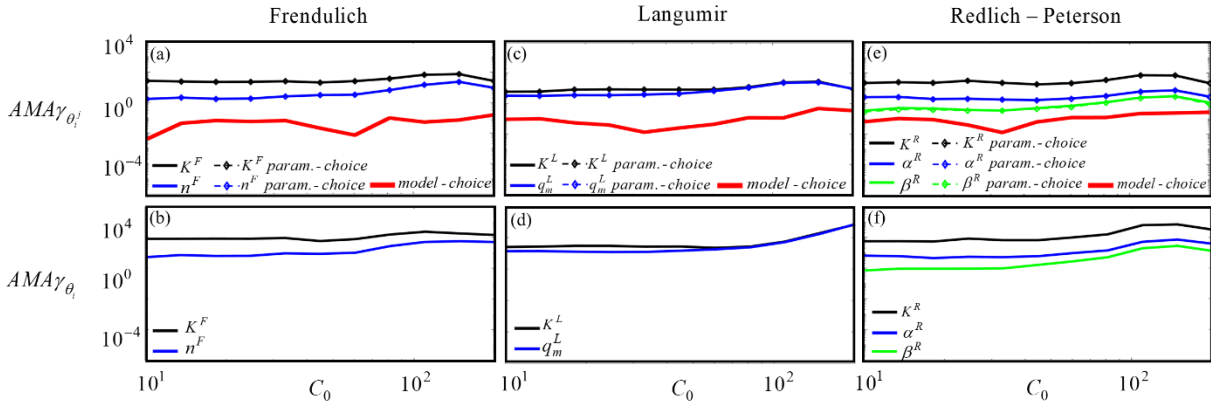
1031

1032

1033

1034

**Figure 7.** Constrained scenario. Sensitivity indices (1) associated with the Variance of  $C$  for the multi-model context versus  $C_0$  considering (a) the Freundlich ( $AMAE_{K^F}$ , black continuous curve, and  $AMAE_{n^F}$ , blue continuous curve); (c) the Langumir ( $AMAE_{K^L}$ , black continuous curve, and  $AMAE_{q_m^L}$ , blue continuous curve); (e) the Redlich-Peterson ( $AMAE_{K^R}$ , black continuous curve,  $AMAE_{\alpha^R}$ , blue continuous curve, and  $AMAE_{\beta^R}$ , green continuous curve). For each index the corresponding (i) parameter-choice contribution (symbols) and (ii) the model-choice contribution (red curves) are also depicted. The counterparts for the single-model context are depicted for (b) the Freundlich, (d) the Langumir and (f) the Redlich-Peterson model.



1035

1036

1037

1038

1039

1040

1041

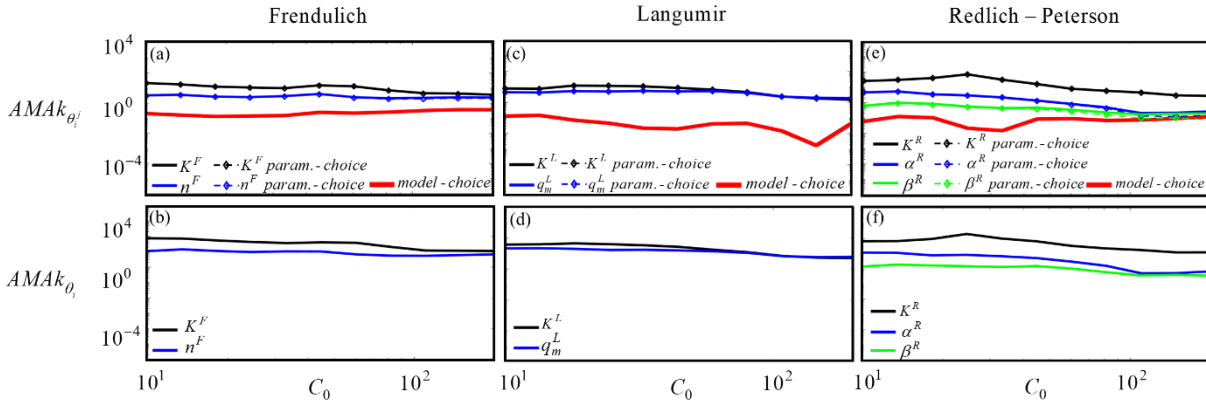
1042

1043

1044

**Figure A.1.** Unconstrained scenario. Sensitivity indices in (1) associated with the skewness of  $C$  for the multi-model context versus  $C_0$  considering (a) the Freundlich ( $AMA\gamma_{K^F}$ , black continuous curve, and  $AMA\gamma_{n^F}$ , blue continuous curve); (c) the Langumir ( $AMA\gamma_{K^L}$ , black continuous curve, and  $AMA\gamma_{q_m^L}$ , blue continuous curve); (e) the Redlich-Peterson ( $AMA\gamma_{K^R}$ , black continuous curve,  $AMA\gamma_{\alpha^R}$ , blue continuous curve, and  $AMA\gamma_{\beta^R}$ , green continuous curve). For each index the corresponding (i) parameter-choice contribution (symbols) and (ii) the model-choice contribution (red curves) of each model, are also depicted. The counterparts for the single-model context are depicted for (b) the Freundlich, (d) the Langumir and (f) the Redlich-Peterson model.





1045

1046

1047

1048

1049

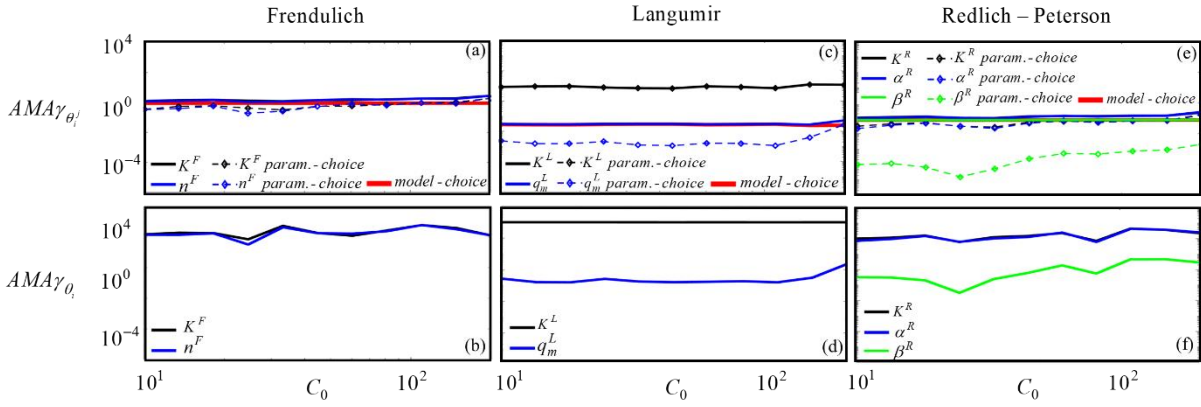
1050

1051

1052

1053

**Figure A.2.** Unconstrained scenario. Sensitivity indices in (1) associated with the kurtosis of  $C$  for the multi-model context versus  $C_0$  considering (a) the Freundlich ( $AMAk_{K^F}$ , black continuous curve, and  $AMAk_{n^F}$ , blue continuous curve); (c) the Langumir ( $AMAk_{K^L}$ , black continuous curve, and  $AMAk_{q_m^L}$ , blue continuous curve); (e) the Redlich-Peterson ( $AMAk_{K^R}$ , black continuous curve,  $AMAk_{\alpha^R}$ , blue continuous curve, and  $AMAk_{\beta^R}$ , green continuous curve). For each index the corresponding (i) parameter-choice contribution (symbols) and (ii) the model-choice contribution (red curves) of each model, are also depicted. The counterparts for the single-model context are depicted for (b) the Freundlich, (d) the Langumir and (f) the Redlich-Peterson model.



1054

1055

1056

1057

1058

1059

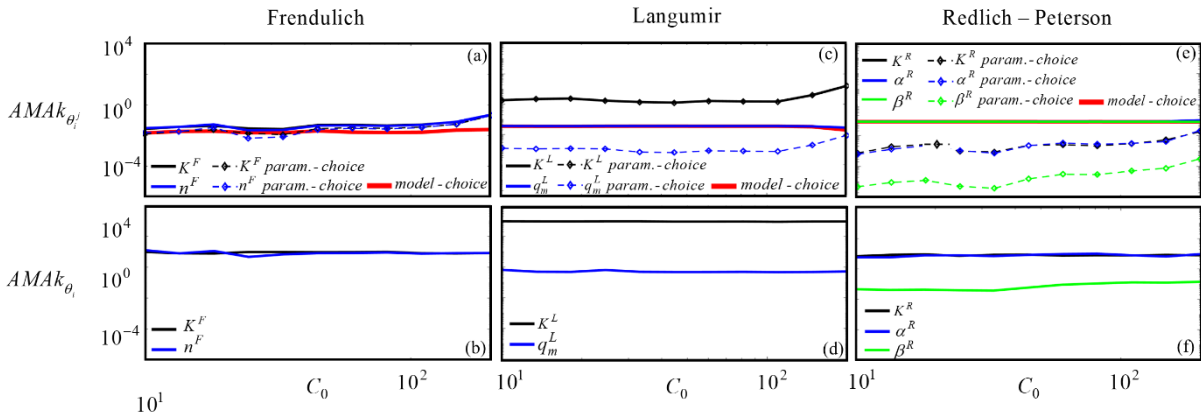
1060

1061

1062

1063

**Figure A.3.** Constrained scenario. Sensitivity indices in (1) associated with the skewness of  $C$  for the multi-model context versus  $C_0$ , considering (a) the Freundlich ( $AMA\gamma_{K^F}$ , black continuous curve, and  $AMA\gamma_{n^F}$ , blue continuous curve); (c) the Langumir ( $AMA\gamma_{K^L}$ , black continuous curve, and  $AMA\gamma_{q_m^L}$ , blue continuous curve); (e) the Redlich-Peterson ( $AMA\gamma_{K^R}$ , black continuous curve,  $AMA\gamma_{\alpha^R}$ , blue continuous curve, and  $AMA\gamma_{\beta^R}$ , green continuous curve). For each index the corresponding (i) parameter-choice contribution (symbols) and (ii) the model-choice contribution (red curves) of each model, are also depicted. The counterparts for the single-model context are depicted for (b) the Freundlich, (d) the Langumir and (f) the Redlich-Peterson model.



1065

1066

1067

1068

1069

1070

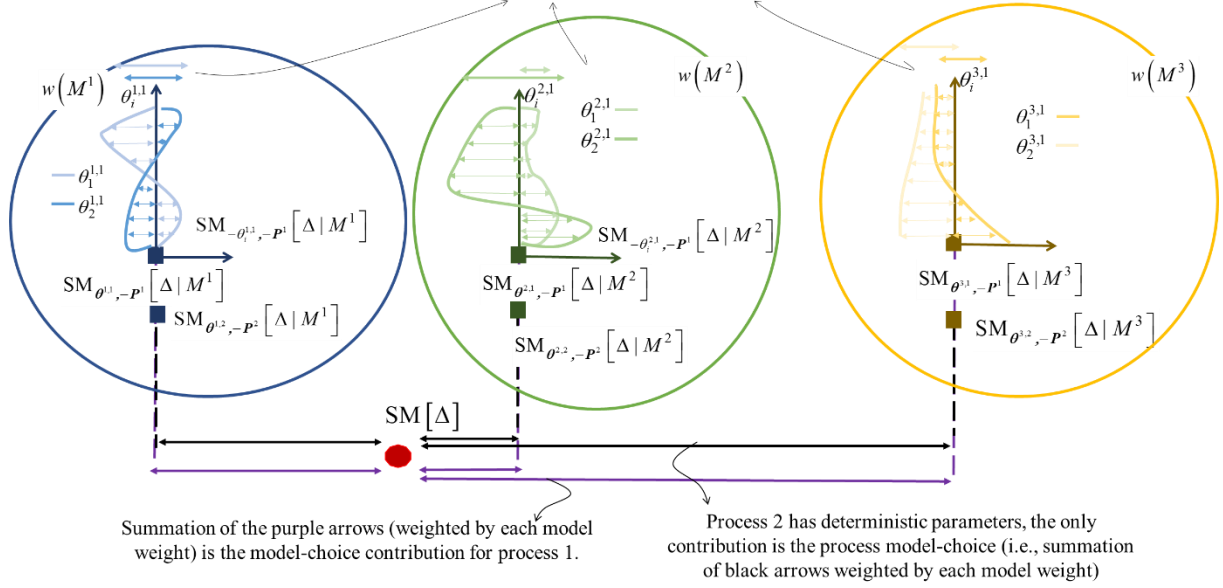
1071

1072

1073

**Figure A.4.** Constrained scenario. Sensitivity indices in (1) associated with the kurtosis of  $C$  for the multi-model context versus  $C_0$  considering (a) the Freundlich ( $AMAk_{K^F}$ , black continuous curve, and  $AMAk_{n^F}$ , blue continuous curve); (c) the Langumir ( $AMAk_{K^L}$ , black continuous curve, and  $AMAk_{q_m^L}$ , blue continuous curve); (e) the Redlich-Peterson ( $AMAk_{K^R}$ , black continuous curve,  $AMAk_{\alpha^R}$ , blue continuous curve, and  $AMAk_{\beta^R}$ , green continuous curve). For each index the corresponding (i) parameter-choice contribution (symbols) and (ii) the model-choice contribution (red curves) of each model, are also depicted. The counterparts for the single-model context are depicted for (b) the Freundlich, (d) the Langumir and (f) the Redlich-Peterson model.

Summation over the (averaged) variability due to lack of knowledge about process 1 parameters gives the parameter-choice contribution.



1074

1075 **Figure D.1.** Sketch of the overall concept underpinning the sensitivity indices  $AMASM_{P^k}$  in (B.2)

1076 , considering the generic statistical moment  $SM$  for the quantity of interest  $\Delta$ . For ease of

1077 illustration we consider only two processes, i.e.,  $P^k$  with  $k = (1, 2)$ . Three distinct

1078 conceptualizations for process  $P^1$  are considered, each characterized by two parameters, i.e.,  $i = (1,$   
 1079  $2)$ , affected by uncertainty, i.e.,  $\theta_i^{j,1}$ . Otherwise, only one conceptualization is considered for

1080 process  $P^2$ , whose parameters are taken to be deterministic. This gives rise to three distinct

1081 models, i.e.,  $j = (1, 2, 3)$ , each with its model-weight, i.e.,  $w(M^j)$ .  $SM[\Delta]$  is the ensuing  $SM$  once

1082 uncertainty in all processes and associated parameters has been accommodated;

1083  $SM_{\theta^{j,k}; P^{j,k}}[\Delta | M^j]$  is the target  $SM$  once uncertainty in the parameters of the  $k$ -th process in  
 1084 model  $M_j$  has been accommodated, the variability associated with other process components

1085 having been averaged out;  $SM_{\theta_i^{j,k}; P^{j,k}}[\Delta | M^j]$  is the target  $SM$  conditioned to  $\theta_i^{j,k}$  of process

1086  $P^k$  and given  $M^j$ , while the variability associated with the remaining parameter of  $P^k$  given  $M_j$

1087 has been averaged out.

1088